REGIONAL COPPER-NICKEL STUDY
CONCENTRATIONS OF MINERAL FIBERS IN PROCESS SAMPLES FROM NORTHEAST MINNESOTA

Minnesota Environmental Quality Board
Regional Copper-Nickel Study
Author: Robert J. Stevenson

November, 1978

INTRODUCTION TO THE REGIONAL COPPER-NICKEL STUDY

The Regional Copper-Nickel Environmental Impact Study is a comprehensive examination of the potential cumulative environmental, social, and economic impacts of copper-nickel mineral development in northeastern Minnesota. This study is being conducted for the Minnesota Legislature and state Executive Branch agencies, under the direction of the Minnesota Environmental Quality Board (MEQB) and with the funding, review, and concurrence of the Legislative Commission on Minnesota Resources.

A region along the surface contact of the Duluth Complex in St. Louis and Lake counties in northeastern Minnesota contains a major domestic resource of copper-nickel sulfide mineralization. This region has been explored by several mineral resource development companies for more than twenty years, and recently two firms, AMAX and International Nickel Company, have considered commercial operations. These exploration and mine planning activities indicate the potential establishment of a new mining and processing industry in Minnesota. In addition, these activities indicate the need for a comprehensive environmental, social, and economic analysis by the state in order to consider the cumulative regional implications of this new industry and to provide adequate information for future state policy review and development. In January, 1976, the MEQB organized and initiated the Regional Copper-Nickel Study.

The major objectives of the Regional Copper-Nickel Study are: 1) to characterize the region in its pre-copper-nickel development state; 2) to identify and describe the probable technologies which may be used to exploit the mineral resource and to convert it into salable commodities; 3) to identify and assess the impacts of primary copper-nickel development and secondary regional growth; 4) to conceptualize alternative degrees of regional copper-nickel development; and 5) to assess the cumulative environmental, social, and economic impacts of such hypothetical developments. The Regional Study is a scientific information gathering and analysis effort and will not present subjective social judgements on whether, where, when, or how copper-nickel development should or should not proceed. In addition, the Study will not make or propose state policy pertaining to copper-nickel development.

The Minnesota Environmental Quality Board is a state agency responsible for the implementation of the Minnesota Environmental Policy Act and promotes cooperation between state agencies on environmental matters. The Regional Copper-Nickel Study is an ad hoc effort of the MEQB and future regulatory and site specific environmental impact studies will most likely be the responsibility of the Minnesota Department of Natural Resources and the Minnesota Pollution Control Agency.

ABSTRACT

The Regional Study includes investigations of the problem of generation of mineral fibers during processing of copper-nickel ores from the gabbroic rocks at the base of the Duluth Complex in northeastern Minnesota. The term fiber is used here in reference to any mineral particle with an aspect ratio greater than three to one. In addition to the Regional Study staff, the Minnesota Department of Health (MDNR), the Mineral Resource Research Center (MRRC), and the Minnesota Geological Survey (MGS) have all cooperated in this study.

The study is based on selected samples from 225 kg splits of nine different occurrences of mineralized gabbro. Thin section modes on an average of 35 thin sections per sample show that the amount of amphibole present varies from below detectable limits (0.01) to approximately 13 volume percent with an average of 2.3 volume percent. The amphibole present in the samples include hornblende, actinolite, and cummingtonite-grunerite. Although no obvious asbestiform habit was found in the nine process samples, an unusual actinolite with asbestiform habit was found in gabbroic rocks adjacent to one of the samples. Other major minerals present in the samples include plagioclase, olivine, pyroxene, chlorite, biotite, copper-nickel sulfides, and iron-titanium oxides.

Using the nine samples, MRRC conducted bench-scale ore concentration tests. Samples of tailing slurries were agitated and then sampled using a standard sedimentation sizing technique with an Andefssen pipette to exclude large fragments. Samples were sent to MDH for fiber analysis. The particles were collected on Nucleopore filters at MDH and were prepared for transmission electron microscopy using the Jaffe-Wick method. The MDH Hitachi model HU12A TEM with tilting stage and attached x-ray energy dispersive analysis system was used for fiber counting. Other samples analyzed for fiber content include: ground feed, concentrate, and tailings generated from a different grinding system, and a series of sedimentation sizing samples derived from one tailing slurry by sampling at various time intervals up to 48 hours after agitation.

Results of the fiber analysis show a good ($r=0.998$) linear fit to a plot of amphibole content by volume from thin section work versus the number of fibers present per liter of slurry following processing. A coarser grinding system produced a fair ($r=0.739$) linear fit. Additional results, although preliminary, indicate a poor linear fit for plagioclase fibers versus plagioclase in the rock samples. Other preliminary work indicates the average aspect ratio for 176 amphibole fibers is 9.18, whereas the average for 110 plagioclase fibers is 7.47. The ranges for the number of amphibole fibers per liter in tailing slurry samples is 4.92×10^{10} to 1.06×10^{13}.

TABLE OF CONTENTS

I. INTRODUCTION

The mineral fiber generation investigation undertaken by the Study was designed to elucidate the number and kind of mineral fibers generated in the processing of copper-nickel ores from the gabbro rocks at the base of the Duluth Complex in northeastern Minnesota. For the purpose of this study, a fiber is defined as an inorganic mineral with parallel sides and an aspect ration (length/width) greater than 3. This definition includes asbestiform material as well as acicular crystals and cleavage fragments. A more detailed discussion of definitions used is given in Appendix I, which is excerpted from the Regional Copper-Nickel Study document, Ambient Concentrations of Mineral Fibers in Air and Water in Northeast Minnesota (Ashbrook 1978). In addition to the Project staff, the Minnesota Department of Health (MDH), the Minnesota Department of Natural Resources (MDNR), the Mineral Resource Research Center (MRRC), and the Minnesota Geological Survey (MGS) have all cooperated in this study.

Mineral fibers present a potentially serious, but presently poorly understood, environmental health hazard for the non-occupational population in both Minnesota, as evidenced by the Reserve Mining controversy, and nationwide (Carter 1977). It is because of this potentially serious hazard that the Regional Copper-Nickel Study undertook the task of investigating the mineral fiber generation in the processing of mineralized gabbro.

II. METHODS

The MRRC conducted bench-scale flotation tests on nine different samples of mineralized gabbro selected from several areas along the base of the Duluth Complex (Figure 1). The nine samples shown on Table 1 and Figure 1 were selected

Table 1. Description of Duluth Gabbro samples.

US9001: Mineralized gabbro sample from the U.S. Steel Research Center open pit bulk sample site.

AX9001: Minnamax leach pad (FL-1) sample of lean ore.

AX9002: AMAX shaft composite sample from depths of 1249 feet and 1312 feet.

AX9003: AMAX shaft composite sample from depth of 1338 feet and 1343 feet.

AX9004: AMAX semi-massive, mineralized rock sample from an exploration drift.

AX9005: AMAX mineralized rock sample (from MRRC sample No. 2) from an exploration drift.

DP9002: Mineralized gabbro sample (from the stockpile of gabbro outcroppings at the Dunka Pit.

IP9002: A sample from INCO's Spruce Road test pit site.

IP9003: A sample from INCO's Maturi shaft, from depths of 798 feet to 905 feet.

to be representative of the material that might be mined in a mining operation in the Duluth Gabbro. The samples were chosen with the help of the MDNR and were macroscopically and chemically similar to material that area mining companies have projected as mineable material.

Mineral resource material at the base of the Duluth Gabbro falls into two general categories, semi-massive and disseminated. Semi-massive material is rock with an average of over 4 volume percent total sulfides. Generally, the rock is less altered than the disseminated material and the grains of sulfide are about the same size as the other minerals in the rock. Because semi-massive material is present only locally and in small quantities, the main interest is in the disseminated material which persists over much larger areas.

In the disseminated material, the sulfides occur as interstitial grains to plagioclase and mafic minerals. Lean ore is defined as disseminated ore that is not treatable under present profit considerations but could be mined in the future. The term "ore" implies that the valuable metals contained in the rock can be recovered at a profit. It must be stressed that the term is used here assuming that present or future studies will indicate that mining can proceed profitably. At present there is no copper-nickel "ore" in Minnesota, in the strict sense of the word.

AX90001 is an example of lean ore. Samples US9001, AX9002, AX9003, AX9005, IP9002, and IP9003 represent disseminated ore, whereas DP9002 and AX9004 represent semi-massive ore. Table 2 is a summary of the mineralogy of the samples. The MGS determined the mean volume percent from thin section work. Figure 2 is a boxplot diagram of Table 2. Boxplot diagrams show the minimum, 25th percentile, median, 75th percentile, and maximum values. The box itself is drawn at the 25th

Table 2. Mean mineralogical composition of test samples (volume %).

GABBRO CLASSIFICATION	"LEAN ORE" AX9001	"DISSEMINATED ORE" US9001	AX9002	AX9003	AX9005	IP9002	IP9003	Disseminated Average	"SEMI-MASSIVE ORE" DP9002	AX9004
Plagioclase	59.112	64.881	61.457	47.363	47.403	65.443	66.166	58.786	47.242	47.855
Sericite	2.176	0.188	2.518	1.911	0.245	2.683	0.373	1.320	0.069	0.091
Olivine	10.510	16.173	13.586	18.267	25.841	16.308	17.123	17.883	10.766	1.513
Clinopyroxene	11.185	7.237	6.809	5.024	7.622	3.717	5.689	26.102	2.656	
Orthopyroxene	3.716	1.834	2.882	1.407	2.132	0.231	0.618	1.517	2.315	18.472
Monocrystalline amphibole	3.567	--	0.095	12.255	0.066	1.387	1.055	2.471	--	0.025
Fibrous amphibole	0.288	--	0.335	0.850	--	0.934	0.077	0.366	--	0.024
Chlorite	1.136	1.349	1.950	3.887	1.377	2.078	2.612	2.202	0.403	0.145
Serpentine	0.257	0.097	0.441	0.033	7.659	0.731	0.026	1.498	0.014	--
Iddingsite	0.075	0.172	0.006	0.019	0.194	0.079	0.064	0.090	0.053	--
Talc	--	--	--	--	0.006	0.061	0.463	0.087	--	--
Biotite	1.738	3.785	3.037	3.010	2.431	1.696	1.788	2.624	5.031	4.475
Smectite	0.021	0.051	0.030	0.053	--	0.025	0.026	0.031	--	--
Celadonite	--	--	--	--	--	--	--	--	--	--
Opaques[a]	5.098	4.025	4.776	5.190	4.720	3.474	5.365	4.592	7.923	19.239
Chalcopyrite-cubinite	0.769	0.875	0.962	1.458	1.355	1.403	1.788	1.305	1.341	3.231
Pentlandite	0.037	0.102	0.012	0.113	0.043	0.117	0.025	0.069	0.341	0.161
Pyrrhotite	0.844	0.882	1.093	1.105	0.497	0.953	1.571	1.017	3.073	12.816
Ilmenite-magnetite	3.477	2.164	2.694	2.510	2.885	0.998	1.989	2.197	3.143	2.564
Graphite	--	--	0.015	0.004	--	--	--	0.003	0.025	0.467
Spinel	--	--	0.009	--	--	--	--	0.001	--	--
Myrmewkite	--	0.106	0.042	--	--	0.288	0.065	0.084	--	--
Apatite	0.085	0.075	0.149	0.172	0.346	0.050	0.013	0.134	0.074	0.118
Epidote	0.953	0.017	0.203	0.470	--	0.698	0.322	0.285	--	--
Allanite	--	--	0.090	--	--	0.007	0.051	0.025	--	--
Calcite	0.056	0.007	0.065	0.017	--	0.089	0.077	0.042	0.006	--
Quartz	--	--	--	--	--	--	--	--	--	0.037
Cordierite	0.027	--	1.515	0.106	--	0.013	--	0.272	--	5.350

[a]The value shown for opaques is the sum of the five following values.

and 75th percentile and the line inside the box is the median. In some instances, no line appears within the box, or no box appears, indicating that the mean coincides with one or both of the quartile values, or one or both of the extremes, respectively.

The dominant mineral in the samples is plagioclase (a feldspar). The other major minerals are olivine, clinopyroxene, orthopyroxene, chlorite, biotite, Cu-Ni sulfides (principally cubanite and chalcopyrite), and Fe-Ti oxide. Also present is amphibole from the alternation of olivine and pyroxene. Notice on Figure 2 that the MGS divided the amphibole into two categories. One is mono-crystalline (M. amphibole), i.e. amphibole that is blocky in outline, and the next one which they call fiberous (F. amphibole), but is better described as being acicular amphibole. The distinction between these two categories is not always obvious, so they are combined into a total amphibole category to the right. The mean value for this total amphibole category is 2.3 volume percent, whereas the median is 0.43 volume percent. The range of volume percent of the amphibole is from below detectable limits, probably near 0.01 percent, up to a maximum of a little less than 13 percent.

In an attempt to simulate possible processing conditions each of the nine samples was ground to two finenesses; a coarser 65 mesh grind and a finer 200 mesh grind. (Iwasaki et al. 1978). Of the resulting 18 samples, all 9 of the 200 mesh grind and 3 of the 65 mesh grind were used for the fiber generation study. Samples of rougher flotation tailing slurries produced in bench scale tests were agitated and then sampled using a standard sedimentation sizing technique with an Andressen pipette, to include only particles, minus 37 um (micrometers) in diameter.

Samples of the water with the suspended tailing particles as well as some bulk sample were then sent to the Minnesota Department of Health for fiber analysis. There, the particles were collected on Nucleopore filters and prepared for Tramission Electron Microscopy using the Jaffe-Wick method. A Hitachi model HU12A transmission electron microscope (TEM) with a tilting stage and an attached x-ray energy dispersive analysis system was used for fiber counting. See Ashbrook (1978) for details of the sample preparation and counting methods used.

The actual samples analyzed by MDH are shown with a description of each in Table 3. The samples that are directly comparable are the first 12 samples in Table 3 and AX9002-200 No. 2. Note that AX9002-200 No. 2 and AX9002-200T-1A are samples taken from different subsamples of the same (AX9002) process samples under identical conditions.

Table 4 shows the amphibole, nonamphibole, ambiguous and total fiber concentrations for the samples shown in Table 3. The 95 percent confidence limits are shown in Appendix II. Since the amount of crysotile present was very low, the data for crysotile is only shown in the total fiber column. For a particular fiber to be placed in the amphibole category it had to give an electron diffraction pattern characteristic of amphibole minerals. A fragment with a clearly non-amphibole, non-crysotile diffraction pattern is classified as non-amphibole, non-crysotile. A fragment which clearly has a chrysotile diffraction pattern is classified as chrysotile. Mineral fibers classified as ambiguous have diffraction patterns or chemical ratios which cannot be used to place the fiber in one of the three previous categories.

The mean aspect ratio for each category was calculated by dividing the mean length by the mean width of all the fibers observed in the category. The mean

Table 3. Description of samples analyzed by MDH.

AX9001-200T-1A	200 mesh grind sample of AX9001 tailings slurry at <37 um
US9001-200T-1A	200 mesh grind sample of US9001 tailings slurry at <37 um
AX9002-200T-1A	200 mesh grind sample of AX9002 tailings slurry at <37 um
AX9002-65T-1A	65 mesh grind sample of AX9002 tailings slurry at <37 um
AX9003-200T-1A	200 mesh grind sample of AX9003 tailings slurry at <37 um
AX9005-200T-1A	200 mesh grind sample of AX9005 tailings slurry at <37 um
IP9003-200T-1A	200 mesh grind sample of IP9003 tailings slurry at <37 um
IP9002-200T-1A	200 mesh grind sample of IP9002 tailings slurry at <37 um
IP9002-65T-1A	65 mesh grind sample of IP9002 tailings slurry at <37 um
DP9002-200T-1A	200 mesh grind sample of DP9002 tailings slurry at <37 um
DP9002-65T-1A	65 mesh grind sample of DP9002 tailings slurry at <37 um
AX9004-200T-1A	200 mesh grind sample of AX9004 tailings slurry at <37 um
AX9002-200F	200 mesh grind of AX9002 feed, all sizes
AX9002-200C	200 mesh grind of AX9002 concentrate, at <37 um
AX9002-200T	200 mesh grind of AX9002 tailing slurry, all sizes
AX9002-200 No. 5	200 mesh grid of Ax9002 tailings slurry, at <37 um; following reagitation of the beaker after 90% of the water had been decanted and replaced by distilled water.
AX9002-200 No. 2	200 mesh grind of AX9002 tailings slurry, at <37 um; sample AX9002-200T-1A is the same type of sample
AX9002-200T-1F	200 mesh grind of AX9002 tailings slurry after settling for 24 hours, without agitation.
AX9002-200T-1G	200 mesh grind of AX9002 tailings slurry after settling for 48 hours, without agitation.
AX9002-200T-1H	200 mesh grind of AX9002 tailings slurry after settling for 48 hours, reagitating and taking a <37 um.
AX9002-200T-1J	MRRC distilled water sample.

Table 4. Concentrations of fibers.

SAMPLE	FIBERS PER LITER X 10^{12} (Number of Fibers) Amphibole	Non-Amphibole	Ambiguous	Total
AX9001-200T-1A	3.03 (39) 7.32[a]	0.774 (10) 5.80	0.852 (11) 6.57	4.65 (60) 7.05
US9001-200T-1A	0.230 (11) 6.96	0.546 (26) 5.21	0.357 (17) 6.06	1.13 (54) 5.56
AX9002-200T-1A	0.588 (29) 5.51	0.912 (45) 5.04	0.366 (18) 7.75	1.86 (92) 5.48
AX9002-65T-1A	0.585 (9) 6.15	1.63 (25) 5.11	0.717 (11) 5.57	2.93 (45) 5.27
AX9003-200T-1A	10.6 (34) 6.84	5.31 (17) 7.06	1.87 (6) 13.14	18.1 (58)* 6.77
AX9005-200T-1A	0.414 (10) 6.84	0.867 (17) 8.72	0.414 (10) 7.00	1.69 (41) 8.59
IP9003-200T-1A	1.64 (16) 11.46	1.43 (14) 7.12	0.819 (8) 8.80	3.96 (38) 8.87
IP9002-200T-1A	1.88 (10) 7.77	2.63 (14) 4.94	4.32 (23) 10.22	8.85 (47) 7.58
IP9002-65T-1A	0.675 (16) 11.04	0.675 (16) 7.79	0.591 (14) 21.14	2.03 (48)** 11.76
DP9002-200T-1A	0.207 (4) 5.53	1.71 (33) 7.62	0.621 (12) 6.23	2.54 (49) 7.36
DP9002-65T-1A	0.0492 (2) 31.71	0.738 (30) 6.11	0.148 (6) 9.00	0.933 (38) 6.94
AX9004-200T-1A	0.182 (4) 4.21	1.23 (27) 4.46	0.318 (7) 4.85	1.73 (38) 4.42
200 mesh grind: range	0.182-10.6	0.546-5.31	0.318-4.32	1.13-18.1
average concentration	2.09	1.71	1.10	4.95
65 mesh grind: range	0.049-0.675	0.675-1.63	0.148-0.591	0.933-2.03
average concentration	0.436	1.01	0.368	1.61

[a]The number shown below fiber concentration is the mean aspect ratio.
*includes one fiber of crysotile
**includes two fibers of crysotile

Table 4 Continued.

FIBERS PER LITER X 10^{12}

SAMPLE	Amphibole	Non-Amphibole	Ambiguous	Total
AX9002-200F				1.24 (54) 6.52
AX9002-200C				1.08 (44) 5.60
AX9002-200T				1.04 (56) 5.68
AX9002-200 No. 5 Tails (90% removed)	3.48 (19) 5.37	3.66 (20) 6.57	1.29 (7) 14.87	8.46 (46) 7.00
AX9002-200 No. 2 Tails	0.570 (13) 6.88	0.660 (15) 5.96	0.483 (11) 7.15	1.71 (39) 6.46
AX9002-200T-1F	0.477 (14) 4.43	0.510 (15) 6.22	0.375 (11) 8.33	1.36 (40) 6.95
AX9002-200T-1G	2.32 (13) 4.53	4.29 (24) 4.04	1.43 (8) 6.00	8.04 (45) 4.50
AX9002-200T-1H	0.981 (8) 5.71	2.08 (17) 4.32	1.83 (15) 4.38	4.89 (40) 4.50
AX9002-200T-1J	0.122×10^{-5}(1) 11.86	0.735×10^{-5}(6) 10.29	1.10×10^{-5}(9) 10.06	2.2×10^{-5}(18)** 10.69

aspect ratio is used in Table 4 so a direct comparison to Ashbrook's document (Ashbrook, 1978) can be made. In the diagrams in the following sections the median aspect ratio will be used because the median provides an estimate of centrality that is less sensitive to non-normality in the data than is the mean. A third way to represent the aspect ratio information is to calculate the mean aspect ratio based on the aspect ratios from each category. Table 5 is a comparison of these three methods. Although the mean method is always high and should not be used, Ashbrook's method does give results that are at the most 25 percent away from the preferred median method.

A calculation (Ashbrook, 1978) of the number of fibers/gram was done for sample AX9002-200T. The concentration found was 1.98×10^9 fibers per gram. This corresponds to an average for the two ≤ 37 um samples (AX9002-200T-1A and AX9002-200 No. 2) of 1.78×10^{12} fibers per liter of water. Therefore, using the conversion factor of 0.00111 and multiplying it times the fibers per liter values shown in Table 4, an approximation of the number of fibers per gram can be made.

The MDH data on the 4 categories of mineral groups can be divided further and the proportions of each main mineral group can be shown. This is done in Tables 6 and 7.

Table 6 shows the percentage splits of the total number of fragments present and the percent of the total which is composed of plagioclase fragments. The plagioclase amounts shown in column 4 are also included in column 2 along with other minerals such as pyroxenes and olivines.

Table 7 shows the percent distribution of the total amount of amphibole present. The three categories of amphibole present in the Duluth gabbro are hornbende, actinolite (tremolite-actinolite series) and cummingtonite (cummingtonite-

Table 5. Representative aspect ratio calculation methods.

	AMPHIBOLE	NONAMPHIBOLE	AMBIGUOUS	TOTAL
Ashbrook, 1978	5.51	5.04	7.75	5.48
Median	5.60	5.24	6.43	5.60
Mean	6.66	6.11	8.37	6.73

Table 6. Fiber percentage of total.

SAMPLE	AMPHIBOLE	NONAMPHIBOLE	AMBIGUOUS	PLAGIOCLASE
AX9001-200T-1A	65.2	16.7	18.3	10.0
US9001-200T-1A	20.0	48.1	31.6	21.8
AX9002-200T-1A	31.6	489	19.6	30.4
AX9002-65-1A	20.0	55.6	24.5	15.6
AX9003-200T-1A	59.7	29.3	10.5	10.3
AX9005-200T-1A	24.5	51.2	24.5	22.0
IP9003-200T-1A	42.0	36.8	21.0	18.4
IP9002-200T-1A	21.3	29.8	48.8	10.6
IP9002-65T-1A	33.3	33.3	29.2	6.3
DP9002-200T-1A	8.2	67.3	24.4	20.4
DP9002-65T-1A	5.3	78.9	15.8	28.9
AX9004-200T-1A	10.5	71.1	18.4	18.4
200 mesh grind:				
range	8.2-65.2	16.7-71.1	10.5-48.8	10.0-30.4
average	31.5	44.4	24.1	18.0
65 mesh grind:				
range	5.3-33.3	33.3-78.91	15.8-29.2	6.3-28.9
average	19.5	55.9	23.2	16.9

Table 6 continued.

SAMPLE	AMPHIBOLE	NONAMPHIBOLE	AMBIGUOUS	PLAGIOCLASE
AX9002-200F	--	--	--	--
AX9002-200C	--	--	--	--
AX9002-200T	--	--	--	--
AX9002-200 No. 5 Tails (90% removed)	41.3	43.5	15.2	19.6
AX9002-200 No. 2 Tails	33.3	38.5	28.2	10.3
AX9002-200T-1F	35.0	37.5	27.5	22.5
AX9002-200T-1G	28.9	53.3	17.8	22.2
AX9002-200T-1H	20.0	42.5	37.5	20.0
AX9002-200T-1J	5.6	33.3	50.0	0.0

Table 7. Distribution of amphibole fibers (%).

SAMPLE	HORNBLENDE	ACTINOLITE+	CUMMINGTONITE	% OF AMPHIBOLE CONTRIBUTION TO TOTAL FIBER COUNT
AX9001-200T-1A	5.1	7.7	87.2	65.2
US9001-200T-1A	36.4	9.1	54.5	20.4
AX9002-200T-1A	31.0	17.2	51.7	31.6
AX9002-65T-1A	33.3	22.2	44.5	20.0
AX9003-200T-1A	23.5	14.7	61.8	59.7
AX9005-200T-1A	40.0	10.0	50.0	24.5
IP9003-200T-1A	18.8	81.2	0.0	42.0
IP9002-200T-1A	87.5	0.0	12.5	21.3
IP9002-65T-1A	42.9	14.2	42.9	33.3
DP9002-200T-1A	0.0	0.0	100.0	8.2
DP9002-65T-1A	100.0	0.0	0.0	5.3
AX9004-200T-1A	25.0	0.0	75.0	10.5
200 mesh grind:				
range	0.0-87.5	0.081.2	0.0-100.0	8.2-65.2
average	29.7	15.5	54.7	31.5
65 mesh grind:				
range	33.3-100.0	0.0-22.2	0.0-42.9	5.3-33.3
average	07W6	YJWd	29.1	19.5
AX9002-200F	--	--	--	--
AX9002-200C	--	--	--	--
AX9002-200T	--	--	--	--
AX9002-200 No. 5 Tails (90% removed)	22.2	22.2	55.61	41.3
AX9002-200T-1F	35.7	7.1	57.2	35.0
AX9002-200T-1G	23.1	23.1	53.8	28.9
AX9002-200T-1H	12.5	25.0	62.5	20.0
AX9002-200T-IJ	0.0	0.0	100.0	5.6

grunerite series). Table 8 summarizes the concentration ranges observed for the various fiber categories in the various sample types.

III. RESULTS AND DISCUSSION

A. Plagioclase

Although plagioclase fibers are not known to be carcinogenic and plagioclase does not crystalize in an asbestiform habit, it will be discussed here because it serves as an illustration of the diagrams that will be used as well as a frame of reference for the following discussions of the amphibole fibers.

Figure 3 is the energy dispersive spectroscopy (EDS) pattern and a photograph from the TEM of a fiber of feldspar. The bar in the right photograph is 1.0 um long. The aspect ratio of the fiber is about 5.6. The gold (Au) peak shown next to the silicon (Si) peak in the EDS photograph results from a coating put over the sample to provide a reference peak.

The range of plagioclase in the tailings water is from 0.12 to 1.8 x 10^{12} fibers per liter. The range of plagioclase in the process sample rocks is from 47.2 to 66.2 volume present. These two quantities are plotted against each other on Figure 4. Although no distinctive linear relation exists between these two quantities, for each sample that has data for the two degrees of grinding, the finer ground sample (200 mesh grind) has more fibers per liter than the coarser 65 mesh grind.

Figure 5 shows the ranges of aspect ratios for the 200 and 65 mesh grind samples. The 200 mesh grind median (5.56) is based on 90 fibers while the 65 mesh grind (also 5.56) is based on 21 fibers. The median aspect ratio for both groups combined is 5.56. it should be mentioned that the median aspect ratio of the 200

Table 8. Summary of fiber concentration ranges.

SAMPLE GROUP	AMPHIBOLE	NONAMPHIBOLE	AMBIGUOUS	TOTAL
10^{12} fibers/liter	min-max	min-max	min-max	min-max
65 grind (3 samples)	0.049-0.675	0.675-1.63	0.148-0.591	0.933-2.03
200 grind (3 samples)	0.207-1.88	0.912-2.63	0.366-4.32	1.86-8.85
200 grind (all samples)	0.182-10.6	0.546-5.31	0.318-4.32	1.13-18.1
10^{9} fibers/gm				
65 grind (3 samples)	0.054-0.747	0.747-1.80	0.164-0.654	1.03-2.25
200 grind (3 samples)	0.229-2.08	1.01-2.91	0.405-4.78	2.06-9.79
200 grind (all samples)	0.201-11.7	0.604-5.87	0.352-4.78	1.25-20.0

mesh grind samples which were taken from the same parent material as the corresponding three 65 mesh grind samples is 5.88. This number is based on a count of 42 fibers. A comparison between the samples is difficult since some of the boxplots are based on as few as 3 fibers. It should also be noted that a number of samples have fibers with aspect ratios greater than 20. High aspect ratios (above 20) are often associated with fibrous or asbestiform material, not material such as plagioclase.

Figure 6 is the histogram of the 65 mesh grind plagioclase aspect ratios. The majority are low, near the MDH's cutoff of 3:1. This relatively low group of aspect ratios is also shown in Figure 7.

Figure 7 is a plot of the length of the fibers in micrometers on the vertical axis versus the width of the fibers in micrometers on the horizontal axis for the plagioclase of the 65 mesh grind system. The median aspect ratio, 5.56, is also shown. The lines shown on the plot are lines of constant aspect ratios; they are presented for reference.

Figure 8 is a plot of the $\log_{10}$ of the aspect ratio (A.R.) on the vertical axis versus the $\log_{10}$ of the length on the horizontal axis. The equations of the lines are as follows:

$$\log_{10} \text{A.R.} = M \log_{10} l + B$$

where A.R. is aspect ratio; l is the length, B is the zero intercept and M is the slope. Wylie (1978) has analyzed four samples of asbestos:

1) A short fiber chrysotile from the New Idria Serpentinite body. Diablo range, California.

2) A long fiber chrysotile from the Jeffrey Mine, Asbestos, Quebec, Canada;

3) An amosite sample consisting of about 95% grunerite asbestos and 5% actinolite asbestos from Africa; and

4) A crocidolite sample (blue asbestos), also from Africa. The two chrysotile samples had not been milled but have been processed to remove impurities. The amosite and crocidolite samples were both air jet milled to reduce the average particle length.

A plot of Wylie's results is shown in Figure 8. Wylie proposed that the slope of the line (M) be considered as a "fibrosity index". The slopes of the lines for the chrysotile samples are close to 1.0 (1.01 and 0.99) while the slope of crocidolite was 0.88 and that of amosite was 0.77. Wylie got excellent correlation coefficients for the lines, all in excess of r = 0.985. Each line is based on between 1200 and 2000 fiber observations. The excellent correlation coefficients are in part due to the method of calculation used. Wylie grouped the data by length increment and calculated an arithmetic mean length and aspect ratio for each increment. The slope and intercept are not affected to any great extent by this increment method, as will be seen below, but one can no longer use the correlation coefficient to get a feel for the distance a particular data point is from the line. Preliminary results by Wylie (1978) on a sample of non-asbestiform massive tremolite suggests an M value of less than 0.5.

Figure 9 is a plot of $\log_{10}$ aspect ratio vs. $\log_{10}$ length of the fibers (21 counts) identified as plagioclase (feldspar) for the three 65 mesh grind samples. The solid line is a fit to all of the data while the dashed line is a fit to the data after the increment method of Wylie (1978) has been applied. The slope or "fibrosity index" of the solid and dashed lines is 0.31 (r = 0.32) and 0.26 (r = 0.56) respectively. Although the r values are low, they are good enough to support the general conclusions that follow. These slope values, as is expected for non-asbestiform material like plagioclase, are well below the slope of the asbestiform samples discussed above.

Figure 10 is the histogram of the 200 mesh grind plagioclase aspect ratios. The majority are low, near the MDH's cutoff of 3:1. Some fibers have higher aspect ratios than were seen in Figure 6. Overall, however, the histogram plots of the two grind methods show that the two systems produce similar aspect ratio distributions. This similarity is also shown in Figure 11.

The distributions in the range of 3 to 6 and 6 to 12 aspect ratio are almost identical between the 200 mesh grind plagioclase (57.8 and 28.9 percent respectively) and the 65 mesh grind plagioclase (61.9 and 28.6 percent respectively) (Figures 7 and 11). The median ratio line, 5.56, is also shown on Figure 11.

Figure 12 is a plot of $\log_{10}$ aspect ration versus $\log_{10}$ length of the fibers (90 counted) identified as plagioclase (feldspar) for the nine 200 mesh grind samples. The solid line is a fit to all of the data while the dashed line is a fit to the data using Wylie's increment method. The "fibrosity index" of the solid and dashed lines is 0.23 ($r = 0.28$) and 0.10 ($r = 0.21$) respectively. The difference in the slopes of the two lines, points out one of the problems of using Wylie's technique; the technique requires a large spread of length, larger than those found in the process samples. The lack of length range in these samples helps explain the relatively low r value. However, even with this drawback, the slopes of the plagioclase lines are obviously not near the value of 1.0 found for asbestiform material.

Although the correlation between volume percent and fibers per liter of plagioclase wasn't good enough to fit a line to the data points, the diagram does show that the finer ground 200 mesh samples produce more fibers per liter than the corresponding 65 mesh samples (Figure 4). Although the median aspect ratio for the two grinds was the same (5.56) there is a small population of fibers with

larger aspect ratios as is seen in Figure 5. The "fibrosity index" of the plagioclase samples is well below even the 0.77 found (Wylie, 1978) for amosite. The "index" for plagioclase is below 0.31 for all methods. The amount of material represented by the counted fibers (MDH didn't count any with an aspect ratio less than 3) will be discussed at the end of the next section.

B. Amphibole

Three types of amphiboles have been identified in the process samples used in the fiber generation study. They are hornblende, actinolite, and cummingtonite.

Figure 13 is an example of hornblende. The EDS spectrum is on the left, showing the principal elements in hornblende, Mg, Al, Si, Ca, and Fe. The photograph to the right is of a fiber of hornblende with an aspect ratio of about 5.1. The bar in the photograph is 0.25 μm long. Figure 14 is an example of actinolite. Note the absence of the alumina peak in the EDS pattern. The aspect ratio of the actinolite shown in the photograph is about 8.5. The bar in the photograph is 0.5 um long. The photographs of the 3 amphibole types shown in Figures 13, 14, and 15 illustrate the median aspect ratios of the 3 groups.

The range for tailings water of the total amphiboles is from 4.92×10^{10} to 1.06×10^{13} fibers per liter. The range of volume percent of amphibole in the process sample rocks is from below detectable limits (0.01) to 13.07 volume percent. These two quantities are plotted against each other in Figure 16. Although the difference in fibers per liter between the two grind methods is not as dramatic as for the plagioclase (Figure 4) the finer ground 200 mesh samples did have a higher concentration of fibers per liter than the corresponding 65 mesh grind. The linearity of the data points for the 65 and 200 mesh grind samples is shown by correlation coefficients (r) of 0.739 and 0.998 respectively.

The position of these two lines also illustrates that the 200 mesh grind produces a higher concentration of fibers in tailings water.

Figure 17 shows the ranges of aspect ratios for the 200 and 65 mesh grind samples. The 200 mesh grind median is based on 155 fibers while the 65 mesh grind is based on 26 fibers. The median aspect ratio for the 200 and 65 mesh grinds is 6.70 and 6.92 respectively, clearly higher than that found for feldspar (5.56). It should also be mentioned that the median aspect ratio of the 200 mesh grind samples which correspond to the three 65 mesh grind samples is 5.89. This number is based on a count of 41 fibers. Recall that the median aspect ratio for these same 200 grind samples of plagioclase is 5.88.

Figure 18 is the histogram of the 65 mesh grind amphibole aspect ratios. Although most of the fibers are close to the 3.0 cutoff, there are more fibers with higher aspect ratios than were present for the plagioclase fibers.

Figure 19 is a plot of length versus width for the 65 mesh grind amphibole. Because of the relatively low number of fibers counted (26), the three amphibole mineral groups are not divided. The total amphibole aspect ratio (6.92) is also shown. This diagram again shows the higher number of higher aspect ratio fibers.

Figure 20 is the $\log_{10}$ aspect ratio versus $\log_{10}$ length plot of the fibers (26 counted) identified as amphibole for the 65 mesh grind samples. The solid line is a fit to all of the data while the dashed line is a fit to the data after the increment method of Wylie (1978). The "fibrosity index" of the solid and dashed lines is 0.31 ($r = 0.28$) and 0.56 ($r = 0.83$) respectively. The 65 mesh grind amphibole plot shown in Figure 20 has the poorest correlation between the two plotting techniques of any of the samples. The reason for this large disparity is unclear. However, even with a slope of 0.56, the fibers of amphi-

bole in the 65 mesh grind samples are still below the values found for asbestiform samples (Wylie, 1978).

Figure 21 is the histogram of the 200 mesh grind amphibole aspect ratios. As was the case with the 65 mesh grind, most of the fibers are close to the 3.0 aspect ratio cutoff. Also, as was the case with the 65 mesh grind, more fibers with higher aspect ratios are present, as compared to the plagioclase samples. This is also shown in Figure 22.

Figure 22 is a plot of length versus width of the 200 mesh grind amphibole fibers. Also shown on Figure 22 are the median aspect ratio lines for the three mineral groups. In an aspect ratio range by range comparison between Figure 19 and Figure 22, the distribution of fibers by range is very similar. Also, when Figures 19 and 22 are taken together and compared to Figures 7 and 11 (plagioclase) there is a shift to higher aspect ratios for the amphiboles as well as a shift by range of percentages to higher aspect ratios.

Figure 23 is a $\log_{10}$ aspect ratio versus $\log_{10}$ length plot of the amphibole fibers (155 counted) for the 200 mesh grind samples. The solid line is a fit to all of the data while the dashed line is a fit to the data using Wylie's increment method. The "fibrosity index" of the solid and dashed lines is 0.26 ($r = 0.29$) and 0.27 ($r = 0.63$) respectively. The agreement of the two lines is much better than it was for the 65 mesh grind amphibole samples (Figure 20). Both slopes are well below those for asbestiform material (Wylie, 1978).

Figures 24, 25 and 26 are length versus width plots of 200 mesh grind hornblende, actinolite, and cummingtonite, respectively. The median aspect ratio lines for the three amphibole mineral groups are also shown on the figures. Although the 200 mesh grind amphiboles as a group have a higher median aspect ratio than the

plagioclase fibers, hornblende has a lower median aspect ratio (5.08) than the 200 mesh grind plagioclase. Actinolite has the highest median aspect ratio (8.46) of all the mineral types while that of cummingtonite (6.70) is the same as the 200 mesh grind amphibole median aspect ratio. The distribution of fibers in the ranges of aspect ratios shown in Figures 24, 25 and 26 also illustrate the point that the three amphibole groups have different fiber populations.

Of additional interest are the proportions of the three amphibole groups present in the 200 mesh grind samples. hornblende, actinolite, and cummingtonite make-up 29.7, 15.5, and 54.7 (Table 7) percent respectively of the amphibole of the 200 mesh grind samples. For the three 65 mesh grind samples, the hornblende, actinolite, and cummingtonite proportions are 58.7, 12.1, and 29.1 (Table 7) percent respectively. A comparison of these last three figures to the respective averages of the corresponding three 200 mesh grind samples (39.5, 10.5 and 54.7) do not show good agreement. However, the proportion of amphibole that makes up total fiber count is 19.5 percent for the three 65 mesh grind samples and 20.4 percent for the three corresponding 200 mesh grind samples. These last two numbers suggest that by increasing the amount of grinding the proportion of, at least, total amphibole doesn't change.

Figures 27, 28, and 29 are $\log_{10}$ aspect ratio versus $\log_{10}$ length plots of the three 200 mesh grind amphibole groups. In all three of these diagrams the solid line is a fit to all of the data while the dashed line is a fit to the data using Wylie's increment method. The hornblende "fibrosity indexes" for the solid and dashed lines are 0.21 ($r = 0.27$) and 0.19 ($r = 0.50$) respectively. In this case the slopes are in close agreement and well below the range given by Wylie (1978) for asbestiform minerals.

The distribution of data in Figure 28 for actinolite gives poor fits for both the solid and dashed lines ($r = 0.18$ and $r = 0.10$ respectively). The slopes ("fibrosity index") of the solid and dashed lines are 0.22 and 0.09 respectively. Even though the slopes of the lines for actinolite are low, as compared to those of asbestiform minerals, the very poor regression coefficients of the lines indicate a need for more information in this case.

Figure 29 is of the cunningtonite which has a "fibrosity index" for the solid and dashed lines of 0.31 ($r = 0.40$) and 0.23 ($r = 0.59$) respectively. In this case the slopes are in fairly close agreement and well below the range given by Wylie (1978) for asbestiform minerals.

As in the case of the plagioclase, the amphibole samples show that for the finer grind system there are more fibers produced (Figure 16). The amphiboles have a higher number of fibers with aspect ratios above 20.0 (Figure 17) than do the plagioclase samples. Considering both methods of data manipulation, the $\log_{10}$ aspect ratio versus $\log_{10}$ length plots indicate that the amphiboles, as is expected, have a higher "fibrosity index" than the respective plagioclase grind systems. The point of interest is, however, that the "indices" for the two mineral groups are quite close; especially when compared to Wylie's (1978) values for asbestiform minerals, and well below Wylie's (1978) values.

A calculation of the average ratio of amphibole to plagioclase in both fibers per liter (2.20 from Table 6) as well as for the composition of the process rock samples (0.048 from Table 2) for the 6 disseminated process samples values gives a rough idea of the fiber forming potential for the two minerals. The resultant value indicates that on the average amphibole formed 46 times as many fibers as an equal amount of plagioclase.

C. AX9002 Time Study Series on Tailing

Besides the fiber analysis of the 200 and 65 mesh grind samples, five additional samples of AX9002 tailings at 200 mesh grind were prepared in order to study the settling characteristics of fibers in tailings slurries.

Figure 30 is the total fiber aspect ratio boxplot of these five samples, plus AX9002-200T1A (see Table 3 for an explanation of the other AX9002-200T samples). Figures 31 and 32 are the plagioclase and amphibole aspect ratio boxplots, respectively, of these samples.

Samples No. 2 and 1A are the same type of sample in that both are from AX9002-200 mesh grind tailings and are the <37 um fraction. A comparison between these two samples on Figures 30, 31 and 32 as well as on Table 3 shows that although the fibers per liter values are very close, sample 1A has consistently lower median aspect ratios as compared to sample No. 2. The range of aspect ratios within 25 percent of the median values is also larger in the No. 2 sample as compared to the 1A sample. Why this is, is not clear. Sample populations may be one contributing factor.

Figures 33-35 and 38-40 are plots of length versus width for amphiboles in these six samples (No. 5, No. 2, 1A, 1F, 1G and 1H). The median aspect ratio difference between samples 1A and No. 2 seen in Figure 32 for amphiboles also shows up in Figure 33 and 34. The distribution by size of the fibers in both figures is quite similar. See below for further size distribution discussion.

Sample No. 5 is a sample of the tailing slurry in which 90% of the supernatant water was decanted and replaced by distilled water after the sample had been allowed to stand for 48 hours. The sample was then agitated and a <37 um sample

taken as usual. Samples No. 1A and No. 2 are normal 37 um samples. The median aspect ratios for sample No. 5 are lower than for sample No. 2 and near or higher than those for sample 1A. Sample No. 5 does contain fibers with high (over 20) aspect ratios. The size distribution seen in the length versus width plot (Figure 35) is similar to those for samples No. 2 and 1A.

Figures 36 and 37 are boxplot diagrams of the lengths of all fibers and amphibole fibers respectively. Samples No. 2 and 1A are close in values in regard to both median length and the width of the distribution for all fibers as well as for amphibole. Sample No. 5 has a similar median length but a wider distribution for all fibers. For amphibole, it has a similar distribution but a much lower median length. This means that in comparison to samples No. 2 and 1A, sample No. 5 has a larger range of fiber lengths, although the median length of the fibers is shorter. Another distinction between sample No. 5 and samples No. 2 and 1A is the higher fiber concentration found in sample No. 5 (Table 4). All fibers categories are higher for No. 5 and the total fiber count is five times that for the No. 2 sample. This indicates that there is a significant trapping of fibers in the tailing sediment. These fibers are not removed with the supernatant water. Upon reagitation, fiber levels in the water equal or exceed previous levels. The reason for the overall increase in fiber concentration here is unclear. It may be that residual process chemicals in the tails increase the ability of the tails to trap and retain fibers. As time passes the chemicals are known to degrade and upon dilution, reagitation and resettling, the fiber-removing efficiency of the sedimentation process may be decreased. This might be particularly true where flocculants are involved.

In order to test whether fibers in solution settle out if left undisturbed, timed samples (1F, 1G, and 1H) were taken from the Andressen Pipette (same sampling

technique as sample 1A) at 24 hours after sample 1A (sample 1F), 48 hours after sample 1A (sample 1G) and 48 hours after 1A but also after agitating the cell to obtain a <37 um sample (sample 1H). The median aspect ratios of samples 1F, 1G, and 1H are shown in Figures 30 through 32. It can be seen that when given an increased time in which to settle the fiber aspect ratios for all fibers (Figure 30) feldspar (Figure 31) and amphibole (Figure 32) are close to the distribution (of the mid 50 percent of fibers) of sample 1A. This similar distribution is also seen in Figures 38-40.

Table 4 also showed no systematic decrease in fiber content of the tailing water with time (samples 1A-1F-1G). if anything, levels appear to increase, consistent with the idea of the release of fibers trapped in the sediments as time passes. The conclusion here is that the data indicates that simply providing adequate settling time in a tailings basin is not a viable means of reducing fiber levels in discharge tailings water.

Of interest in regard to the settling qualities of tailing slurries is the size of the fibers. As is seen in Figures 36 and 37, there is a distinct decrease in the range of fiber length from sample 1A to 1F to 1G. This decrease is shown not ony by the distribution of lengths but also by the median length. The same trend is apparent for the amphibole fibers alone (Figure 37). Sample 1H, the agitated equivalent of sample 1G, shows an increase in distribution range for all fibers (Figure 36) and an increase in median length for all fibers (Figure 36) as well as for amphibole (Figure 37). This would indicate that longer fibers do tend to settle in time. However, they comprise a fairly small fraction of the overall fiber content of the water, so the change is insignificant in terms of total fiber concentration. This may be an important observation; however, since the longer fibers may be of more concern in terms of health implications (see Volume

5-Chapter 2 of the Regional Copper-Nickel Study reports). More work is needed to clarify this settling behavior.

The last sample (AX9002-200T-1J) shown in Table 4 is a sample of distilled water MRRC used in its bench scale tests. The influence of the fiber concentration of the input water is neglected in this study because the concentration level in the water is six orders of magnitude below that of the samples.

Samples AX9002-200F, and AX9002-200T are samples of feed (or ore), and tailings, respectively, of the mineralized Duluth Gabbro sample AX9002 with a 200 mesh grind. These samples differ from the other samples because they were not taken using an Andressen Pipette but rather they are grab samples of all size fraction. Thus, they are not restricted by Stokes' law to being, for example, a <37 um fraction, etc. Sample AX9002-200C is a sample of the concentrate produced from the flotation cell and is a <37 um sample. The concentrations of these 3 samples were determined only for the total fiber category, i.e. the fibers were not split into amphibole, non-amphibole, and ambiguous categories. The concentrations shown in Table 4 are close to each other as well as being close to samples AX9002-200T-1A and AX9002-200 No. 2. The length distribution for all fibers for samples AX9002-200T-1A (1A), AX9002-200T (TAIL), AX9002-200F (FEED), and AX9002-200C (CONC) are shown in Figure 41. As can be seen from the diagram, no correlation between sample and length is present. In fact, for all four samples, the mid 50 percent of the lengths overlap. The low median lengths and large amount of short fibers in the tail and feed (Figure 41) samples are not understood. One possible explanation is in sampling procedures. Recall that samples 1A and "conc" of Figure 41 are samples of the <37 um fraction whereas samples "tail" and "feed" are bulk samples. It is possible that a number of small fibers are being lost by the sampling technique used. One general conclu-

sion is that the samples all contain comparable fiber concentrations. Fibers present in the feed are apparently not selectively concentrated into either the tailing or the concentrate by the flotation process.

IV. CONCLUSIONS

The fiber generation study has found that of the three groups of fibers shown in Table 4, amphibole and plagioclase (from the non-amphibole column) can be used to illustrate trends and probable concentrations in tailing slurry waters.

The median aspect ratio found for amphibole and plagioclase is illustrated in Figures 3, 14, 15 and 16. The non-asbestiform morphology of these fibers as well as the low "fibrosity index" found using the $\log_{10}$ aspect ratio versus $\log_{10}$ length diagrams (Figures 9, 12, 20 and 23) show that the dominant (major influence on Wylie type plots) fiber found in the study is not truly asbestiform but rather an acicular crystal fragment or a cleavage fragment.

The volume percent of plagioclase and amphibole in the rock versus the amount released as fibers upon grinding and processing (Figures 4 and 16) shows that the finer the sample is ground the higher the concentration of fibers (see Figure 16). Table 8 summarizes these values. These figures also show that there is a very good correlation between the volume percent of amphibole in the rock and the concentration produced after processing ($r = 0.998$ for 200 mesh grind amphibole). This correlation is not present for plagioclase probably because of the low representation if fragments that gave an aspect ratio greater than 3 to 1. Recall that from this study, amphibole produces fibers at a rate of 46 times that of plagioclase. Using values from Lee and Fisher (1978) it appears that the plagioclase represented by fragments with an aspect ratio greater than 3 to 1 is less than 2 percent of the total amount of plagioclase fragments present.

Based on Figures 6, 10, 18 and 21, the aspect ratio distribution is similar for the different minerals independent of grinding severity.

The three amphibole groups shown in Figure 22 all have different aspect ratios with actinolite producing the highest at 8.46. This shows that, at least for aspect ratio, the different amphibole groups produce different aspect ratio populations.

Although most of the information produced by the process sample timed study (AX9002 series) is not conclusive, the study did show a higher concentration of fibers following replacement of supernatant with distilled water and reagitating. It also showed a remarkably good agreement in concentration between samples AX9002-200 No. 2 and AX9002-200T-1A. The MRRC distilled water was shown to not be a factor in concentration values and the flotation process was shown not to selectively concentrate fibers into a single output product.

Some comparison should be made between the Duluth Complex fiber generation potential and that of the Peter Mitchell Pit. Figure 42 is a comparison of a sample collected by Bonnichsen (1968) from the Peter Mitchell Pit and a sample from the AMAX test shaft. The samples were collected from sites within 10 miles of each other. Notice that the alteration of the olivine (Ol) to cummingtonite (c) produces the same acicular crystals.

From calculations based on work by Cook et al. (1976) the concentration of amphibole in the tailings produced by Reserve Mining Company are in the range of 5.5×10^{11} to 5.5×10^{13} fibers per liter (6.1×10^{8} to 6.1×10^{10} fibers/gram). The amount of amphibole present in the rock depends on which member or combinations of members of the Biwabik Iron Formation are being mined. The total amphibole content varies between 3 and 10 volume percent (Bonnichsen,

1968). Using a value of 9 percent (the average for the three parts being mined) and using Figure 16, the concentration of amphibole for the two rocks can be compared. The Duluth Complex data show approximately 1/3 the amphibole content of the Biwabik formation. Based on this comparison, the Duluth gabbro will produce, on an average, concentrations of amphibole comparable to or less than those of Reserve Mining Company. A plot of the average amount of amphibole in the disseminated samples is shown on Figure 16.

Recent results by the MDH for a sample of recycled water (cleaned tailing slurry water) (sample number 2002D) show a major drop in amphibole concentration. The sample was taken from a continuous pilot plant processing test run at MRRC on Duluth Complex material containing disseminated Cu-Ni mineralization (Iwasaki, 1978A). Unlike the bench scale process tests run earlier, a flocculant was added to aid in clarification of process water prior to recycling. The amphibole fiber per liter level was only 3.39×10^7, with total fibers at 2.82×10^8 fibers/liter. This indicates that by adding a flocculant (e.g. starch) the concentration of amphibole fibers in the water (they will still be present in the sample but now will have settled out) can be reduced by 4 to 5 orders of magnitude.

REFERENCES CITED

Ashbrook, P., 1978. Ambient concentrations of mineral fibers in air and water in northeastern Minnesota. Regional Copper-Nickel Study Report.

Bonnichsen, B., 1968 General geology and petrology of the metamorphosed Biwabik Iron Formation Dunka River area, Minnesota. Ph.D. thesis, University of Minnesota.

Campbell, W.J. and R.L. Blake, L.L. Brown, E.E. Cather and J.J. Sjoberg, 1977. Selected silicate minerals and their asbestiform varieties. U.S. Bureau of Mines Circular 8751.

Carter, L.J. 1977. Asbestos: trouble in the air from Maryland rock quarry. Science 197:237-240.

Cook, P.M., I.B. Rubin, C.J. Maggiore and W.J. Nicholson. 1976. X-ray diffraction and electron beam analysis of asbestiform minerals in Lake Superior waters. Institute of Electrical and Electronics Engineers. Annals No. 75CH1004-I 34-1 pp. 1-9.

Iwasaki, I., Malicsi, A.S., Lipp, R.J., 1978. Final Report to Minnesota Environmental Quality Board and Copper-Nickel Study. Mineral Processing Studies--Flotaton Tests, Mineral Resources Research Center, University of Minnesota.

Iwasaki, I. 1978A. Letter to Peter Kreisman dated Nov. 6, 1978.

Lee, R.J. and R.M. Fisher. 1978. Identification of fibrous and non-fibrous amphiboles in the electron microscope. NYAS workshop No. 1.

Wylie, A. 1978. Fiber length and aspect ratio of some selected asbestos samples. NYAS workshop No. 1.

APPENDIX I

Asbestos is used as a collective mineralogical term encompassing the asbestiform varieties of various silicate minerals and is applied to a commercial product obtained by mining primarily asbestiform minerals (Campbell, et al. 1977). Five minerals fit this definition: chrysotile (a member of the serpentine group), and the asbestiform varieties of actinolite-tremolite, anthophyllite, cummingtonite-grunerite, and riebeckite (memers of the amphibole group). Chrysotile always occurs in the asbestiform habit, amphiboles usually occur in non-asbestiform habits, with the exception of riebeckite, which usually occurs in the abestiform habit as crocidolite. Asbestiform minerals occur as fibers, which display some resemblances to organic fibers in terms of circular cross section, flexibility, silky surface luster, and other characteristics. Cleavage fragments, such as those produced from crushing and processing non-asbestiform minerals, do not satisfy this definition of fibers and should be considered "fiber-like". When asbestiform and non-abestiform minerals are subjected to crushing and processing, the resulting fragments have minor differences in morphology and physical properties that are very difficult to distinguish under a transmission electron microscope. For this reason, when the transmission electron microscope is used, fibers are defined as fragments with aspect (length to width) ratio of 3:1 or greater, even though many of these fragments may not meet the mineralogic definition of a fiber. In this paper the term "mineral fiber" is used to denote both asbestos fibers and cleavage fragments of non-asbestiform minerals because ambient levels of mineral fibers were determined by transmission electron microscopy, which did not distinguish between these two classifications.

Appendix II. Confidence limits for Table 4 concentrations.

10^{12} Fibers Per Liter, 95% Confidence Limit

SAMPLE	AMPHIBOLE	NONAMPHIBOLE	AMBIGUOUS	TOTAL
AX9001-200T-1A	2.15-4.14	0.372-1.43	0.426-1.52	3.54-5.97
US9001-200T-1A	0.115-0.411	0.357-0.798	0.207-0.573	0.849-1.48
AX9002-200T-1A	0.393-0.786	0.666-1.22	0.216-0.576	1.50-2.28
AX9002-65T-1A	0.268-1.11	1.05-2.40	0.357-1.28	2.14-3.93
AX9003-200T-1A	7.35-14.8	3.09-8.49	0.687-4.08	13.7-23.4
AX9005-200T-1A	0.198-0.759	5.37-13.3	0.198-0.759	1.22-2.30
IP9003-200T-1A	0.94-2.66	0.783-2.41	0.354-1.61	2.75-5.34
IP9002-200T-1A	0.903-3.45	1.44-4.41	2.74-6.48	6.51-11.8
IP9002-65T-1A	0.387-1.10	0.387-1.98	0.324-0.993	1.49-2.69
DP9002-200T-1A	0.056-0.531	1.18-2.40	0.321-1.09	1.88-3.36
DP9002-65T-1A	0.0059-0.178	0.498-1.05	0.054-0.321	0.663-1.28
AX9004-200T-1A	0.050-0.468	0.81-1.79	0.128-0657	1.22-2.38
AX9002-200F				0.86-1.50
AX9002-200C				0.547-0.940
AX9002-200T				0.786-1.45
AX9002-200 No. 5 Tails (90% removed)	2.10-5.46	2.24-5.67	0.516-2.65	6.18-11.3
AX9002-200 No. 2 Tails	0.303-0.978	0.369-1.09	0.241-0.864	1.22-2.34
AX9002-200T-1F	0.260-0.801	0.286-0.843	0.187-0.672	0.975-1.86
AX9002-200T-1G	1.23-3.96	2.75-6.36	0.62-2.81	5.85-10.74
AX9002-200T-1H	0.423-1.93	1.21-3.33	1.03-3.03	3.53-6.66
AX9002-200T-1J	0.0031-0.682×10^{-6}	0.270-1.60×10^{-6}	0.505-2.09×10^{-6}	1.31-3.48×10^{-6}

Figure 1

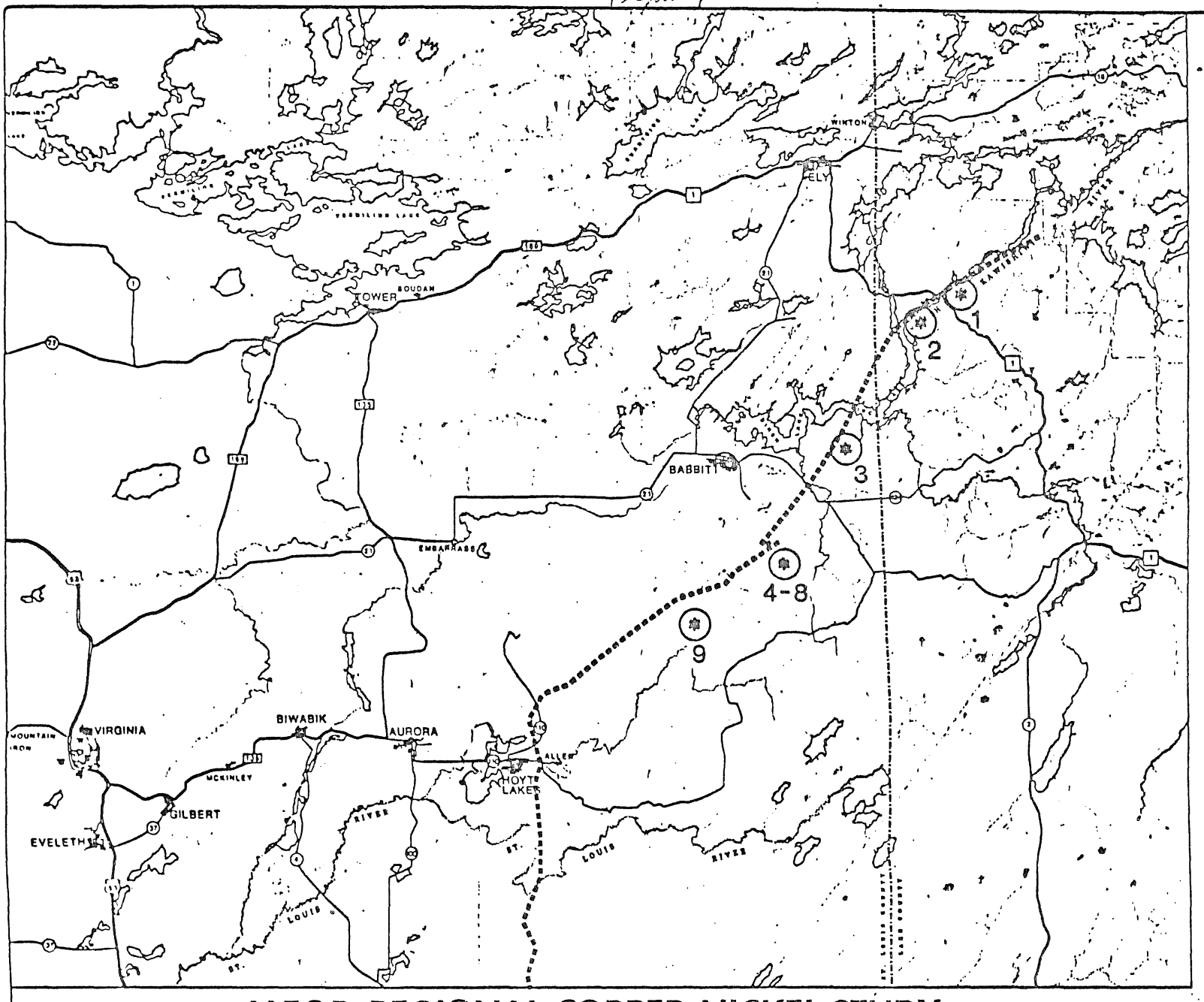

LEGEND

1. IP9002
2. IP9003
3. DP9002
4. AX9001
5. AX9002
6. AX9003
7. AX9004
8. AX9005
9. US9001

DULUTH GABBRO CONTACT

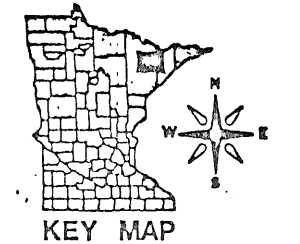

KEY MAP

1:422,400

MILES

KILOMETERS

MEQB REGIONAL COPPER-NICKEL STUDY

FIGURE 1. SAMPLE LOCATIONS

FIGURE 2: Boxplot of mineral compositions of the 9 process samples

Figure 2
Boxplot of mineral compositions of the 9 process samples

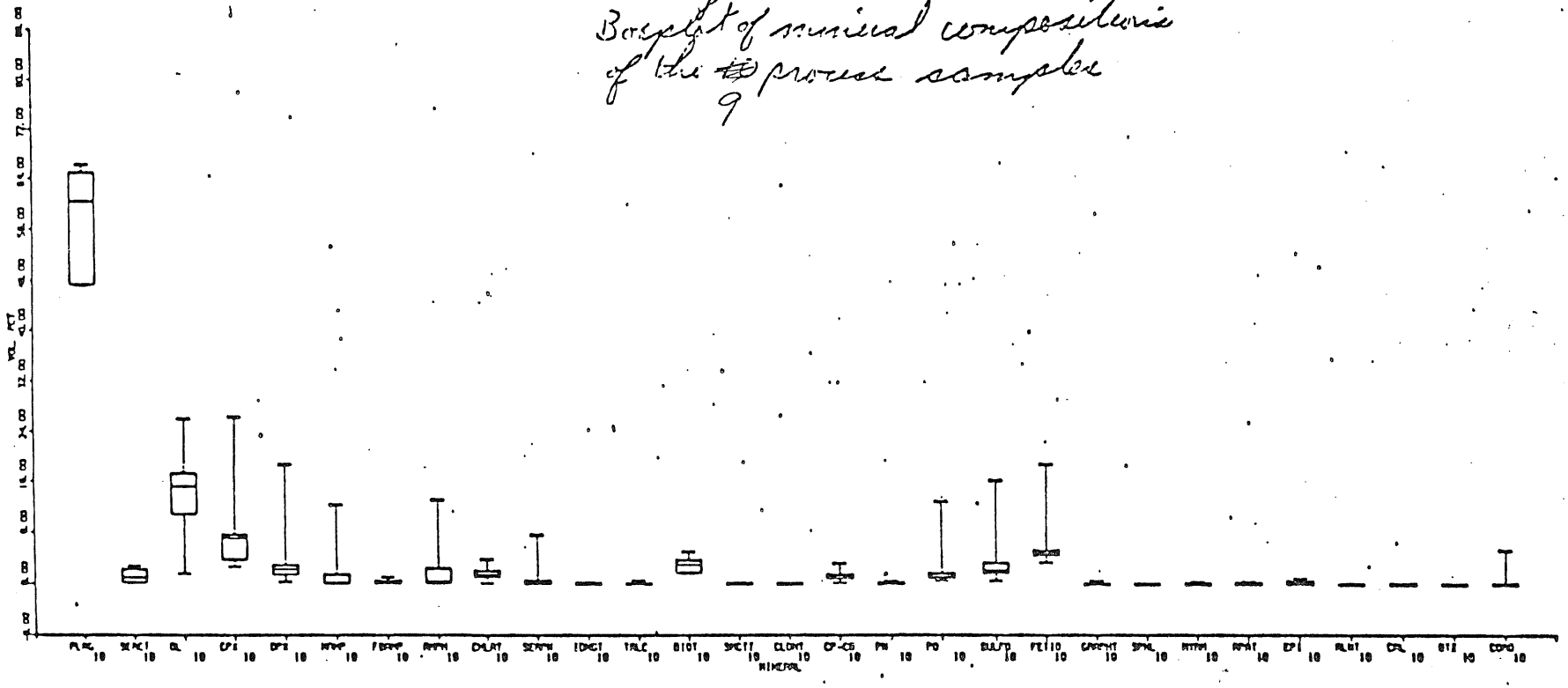

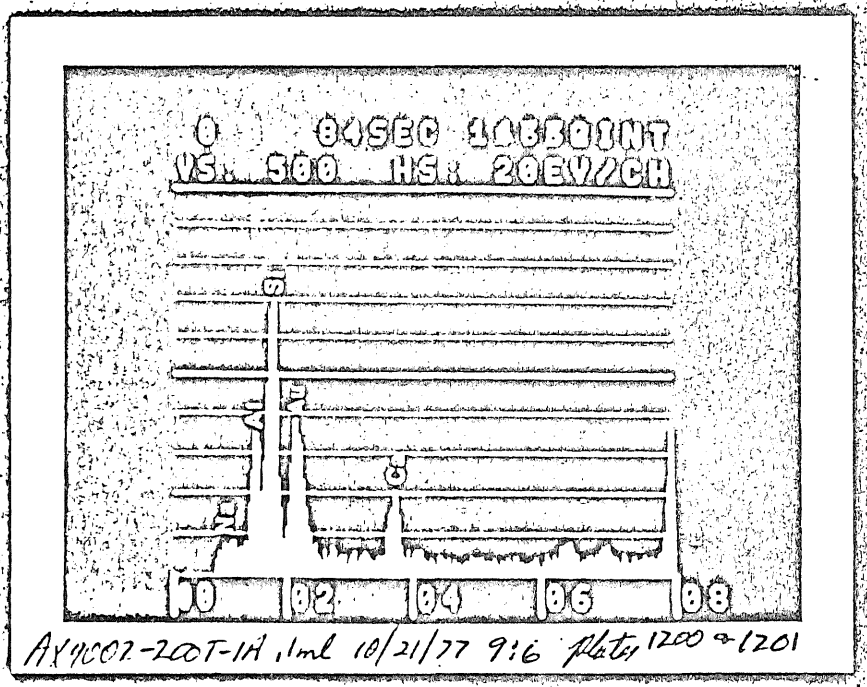

AX4007-20T-1H .1ml 10/21/77 9:6 Plots 1200 & 1201

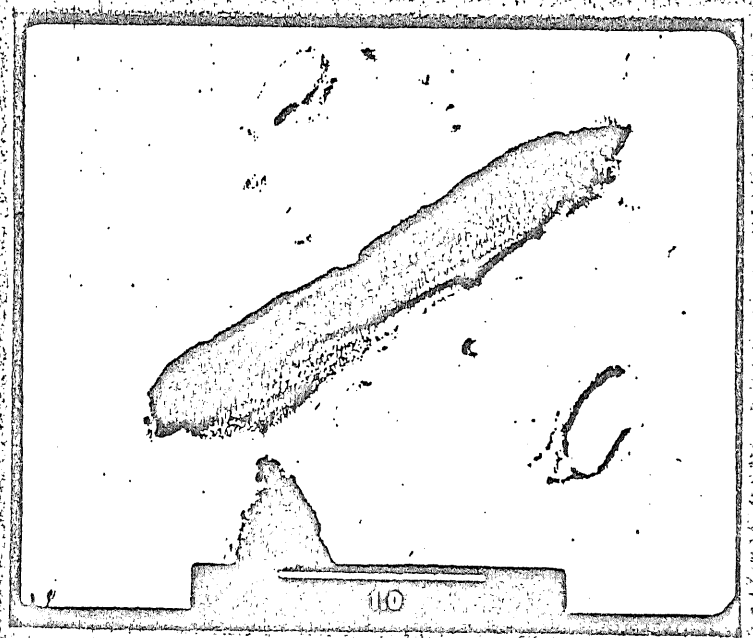

FELDSPAR

Figure 3

Figure 4

PLAGIOCLASE

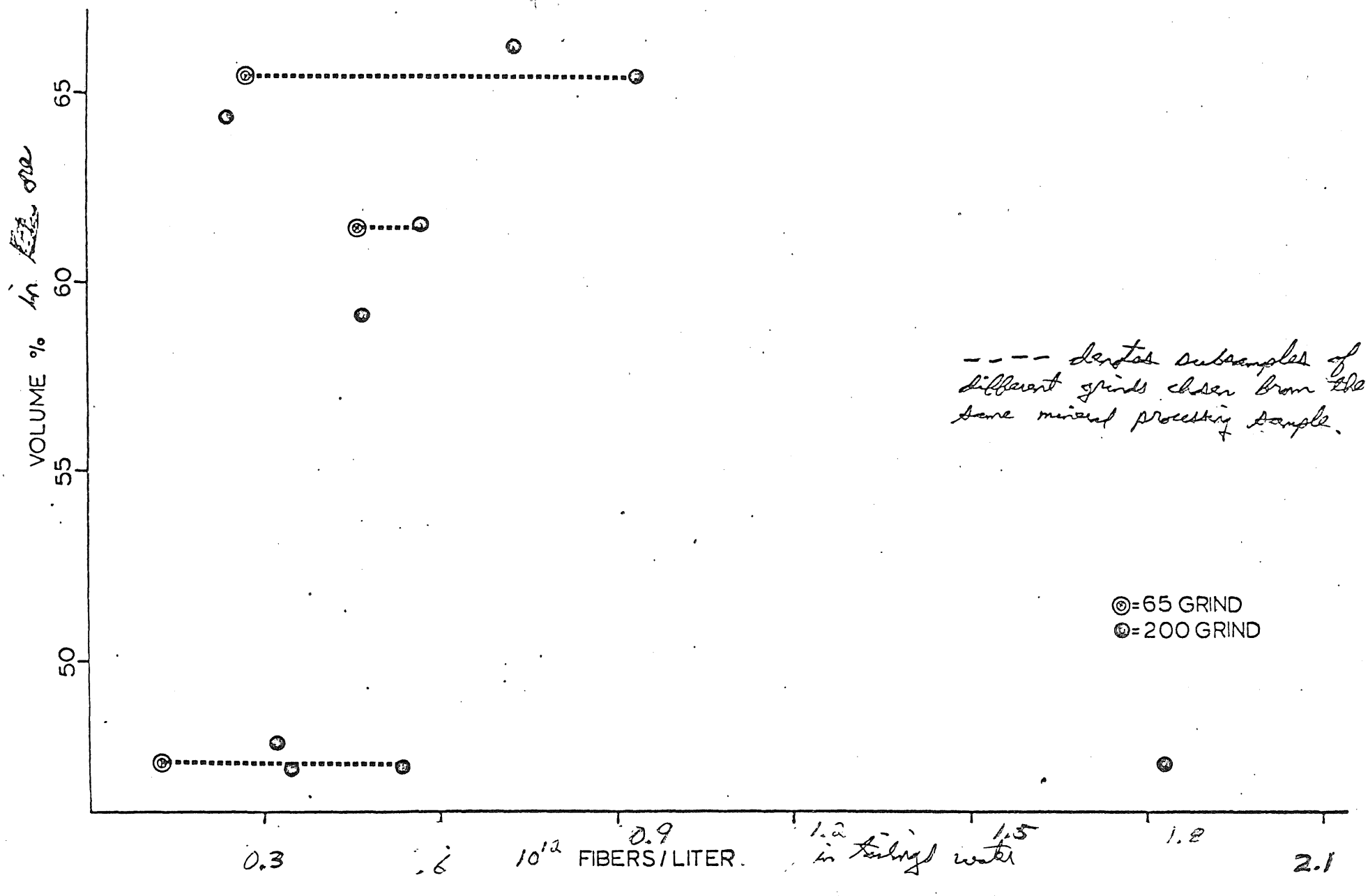

Figure 5

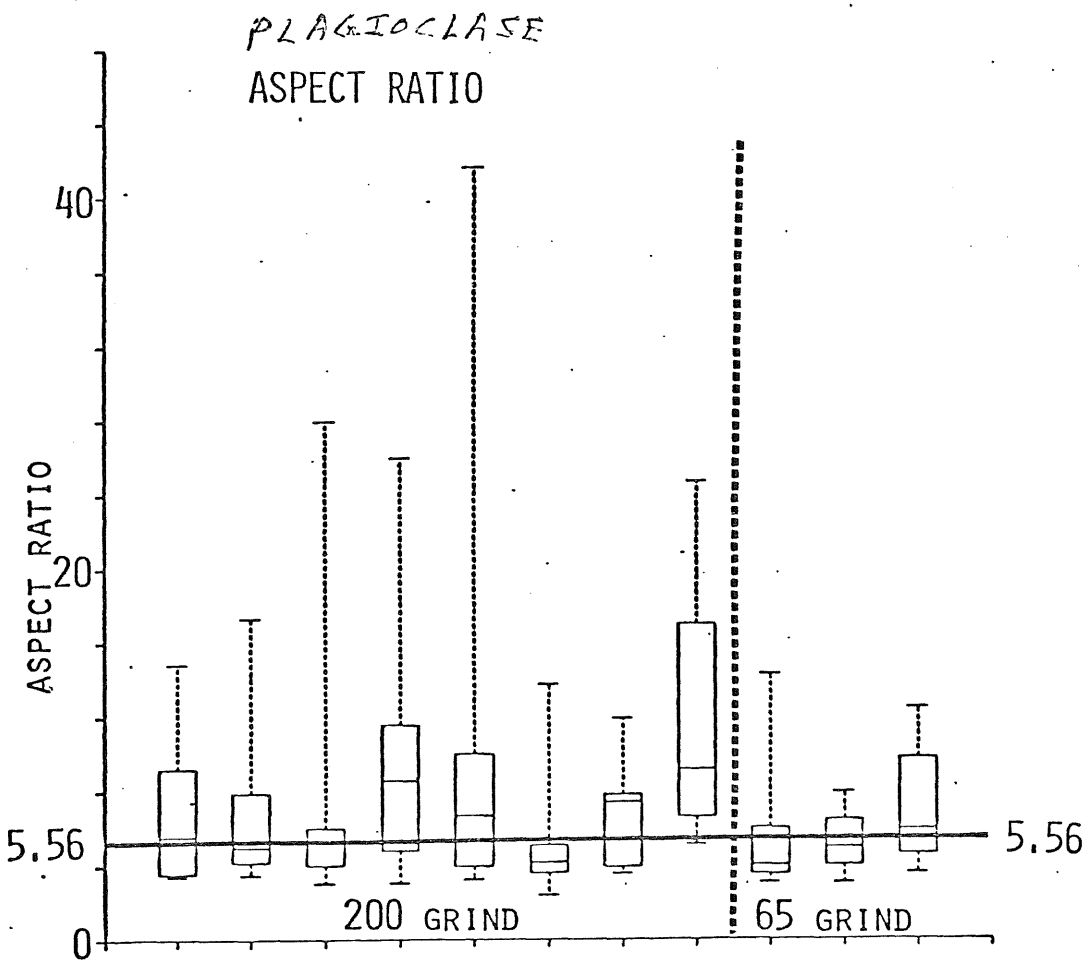
PLAGIOCLASE
ASPECT RATIO
ASPECT RATIO
40
20
0
5.56
5.56
200 GRIND
65 GRIND

Figure 6

PLAGIOCLASE ASPECT RATIO
DISTRIBUTION IN TAILING SAMPLES, 65 mesh grind.

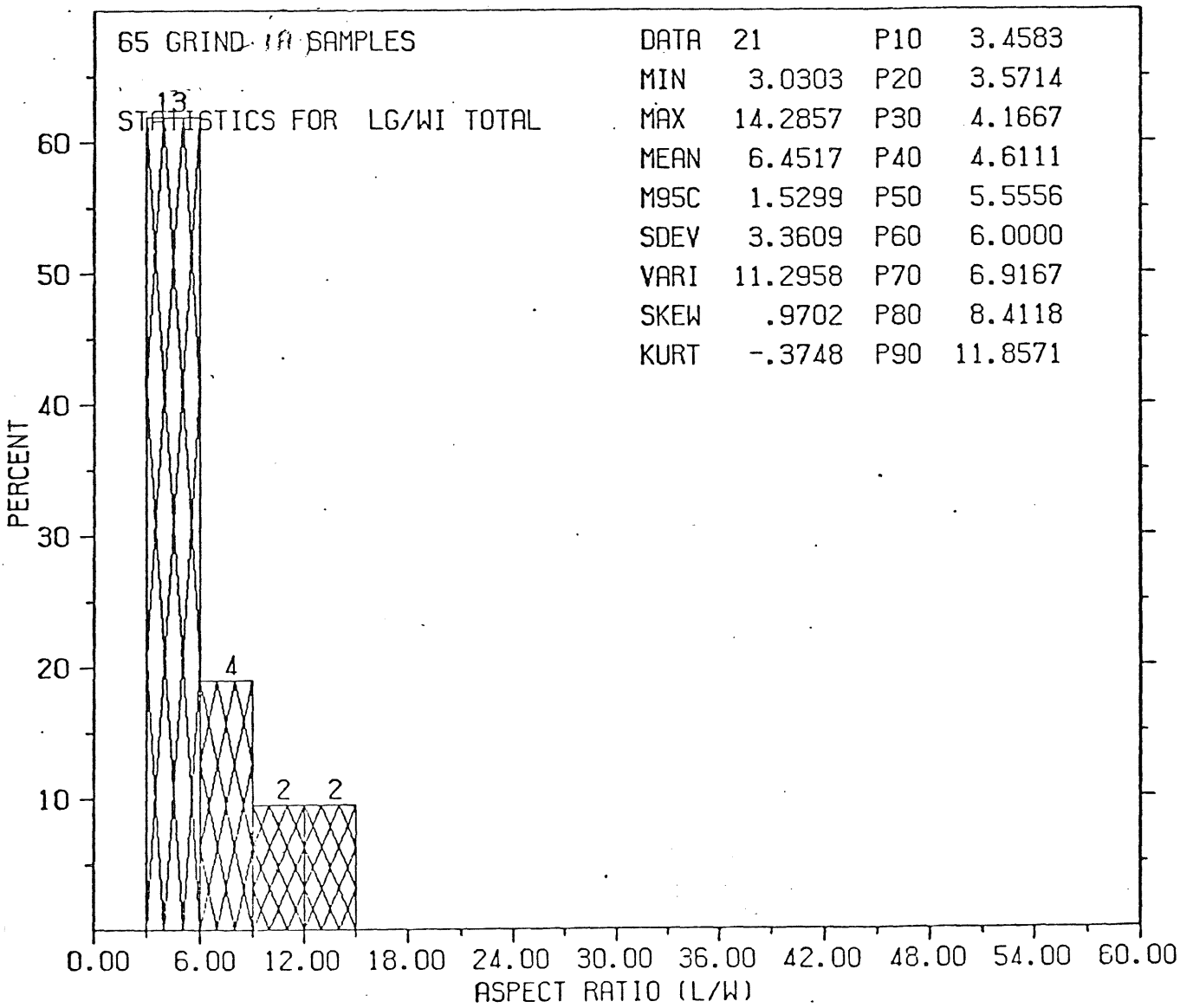

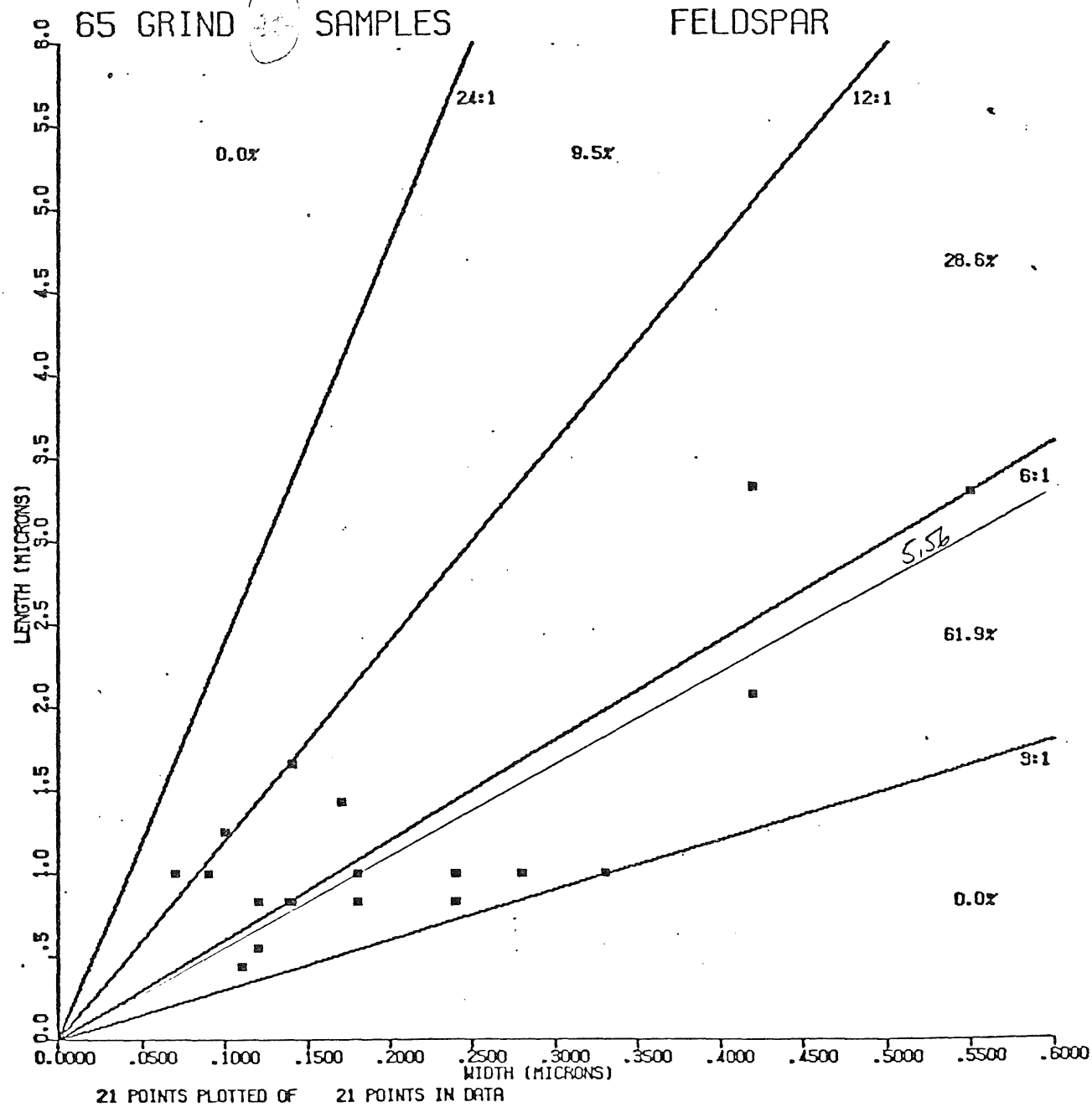

Figure 7 - Plot of length versus width for measured plagioclase fibers in tailing samples, 65 mesh grind.

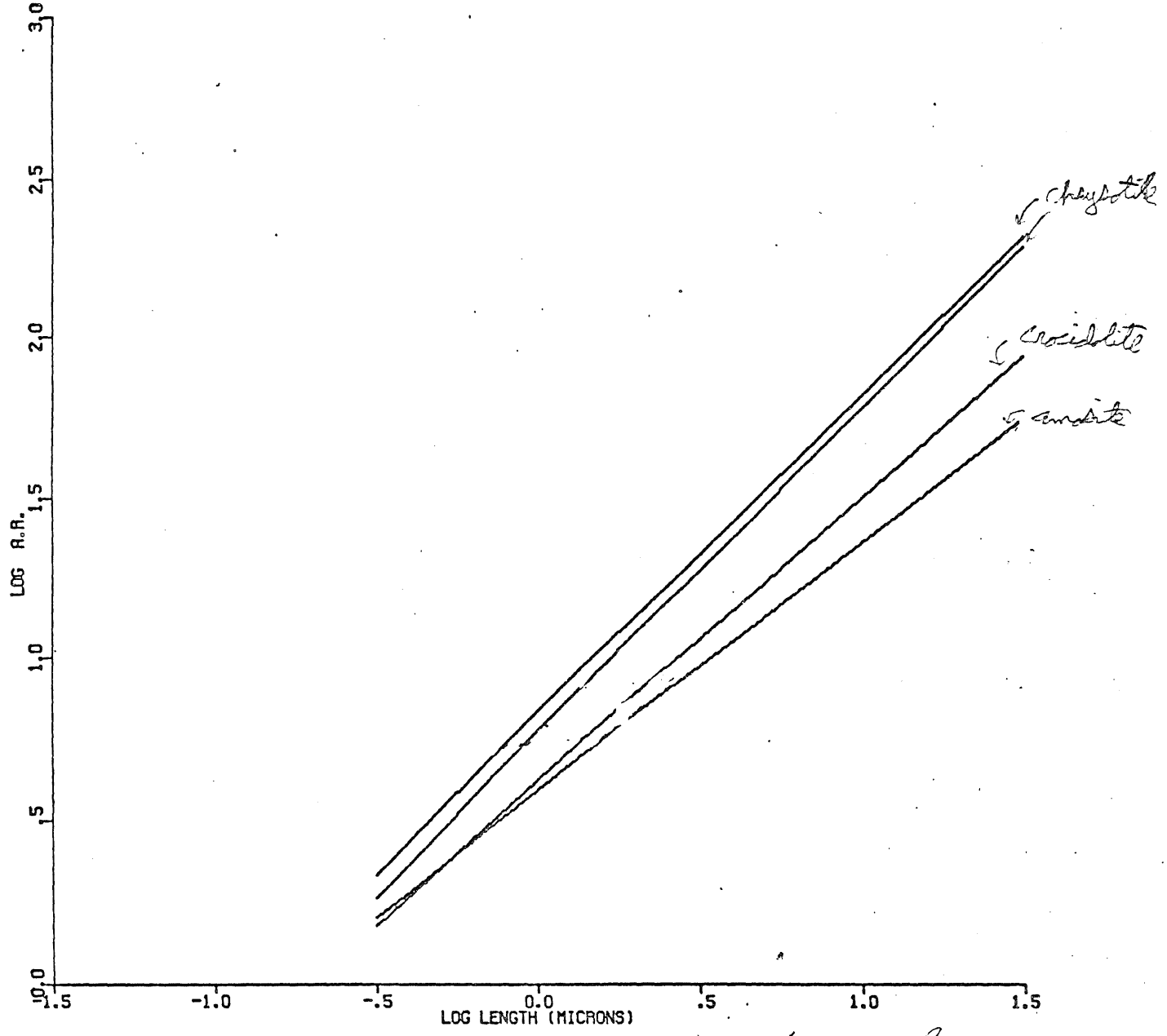

Figure 8: log-log plot of aspect ratio vs. fiber length for four samples of asbestos. (from Wylie, 1979).

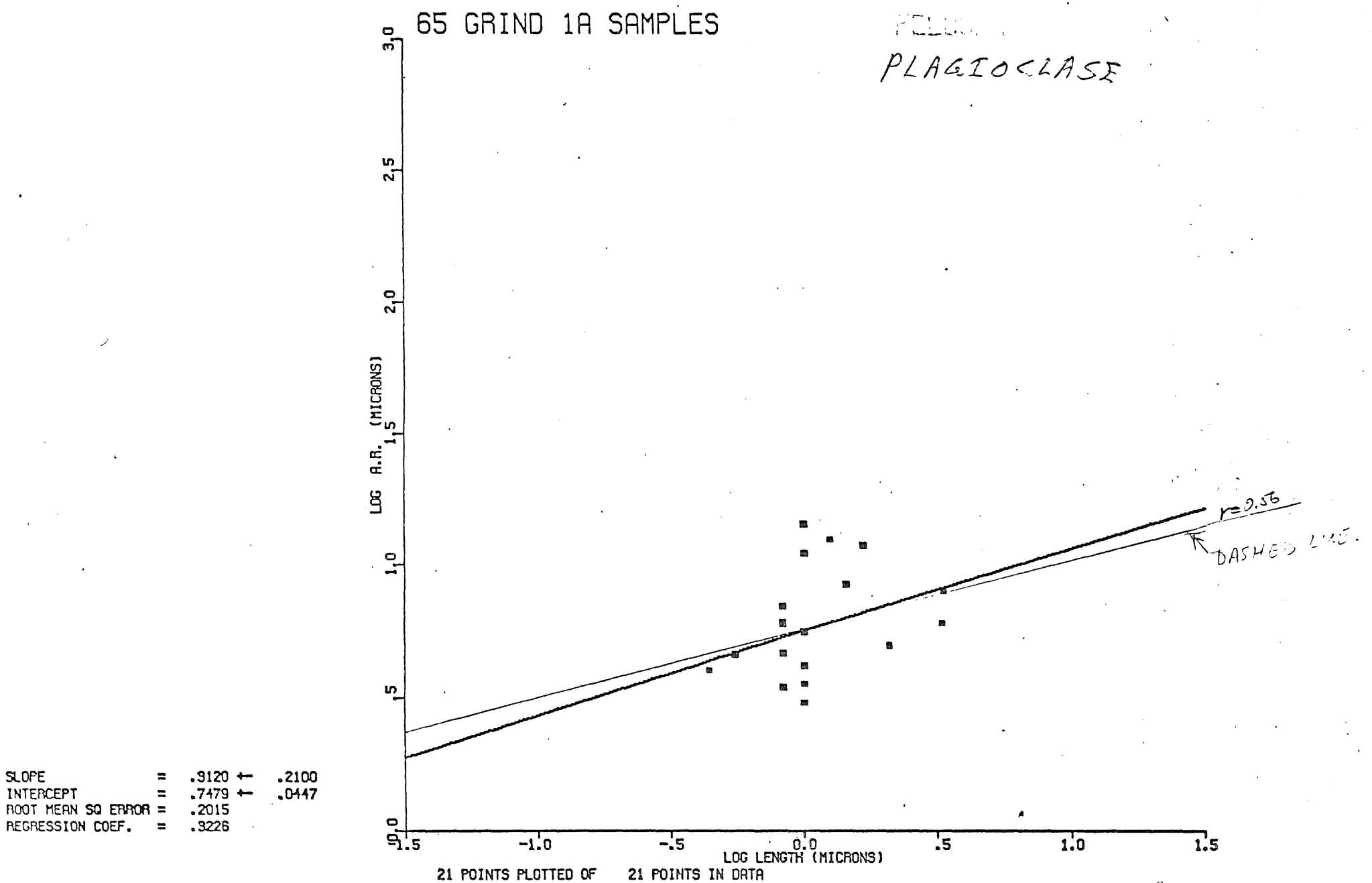

Figure 9: log-log plot of aspect ratio versus fiber length of 21 plagioclase fibers from 3 samples (65 mesh grind tailing).

Figure 10 : Plagioclase aspect ratio distribution in tailing samples, 200 mesh grind.

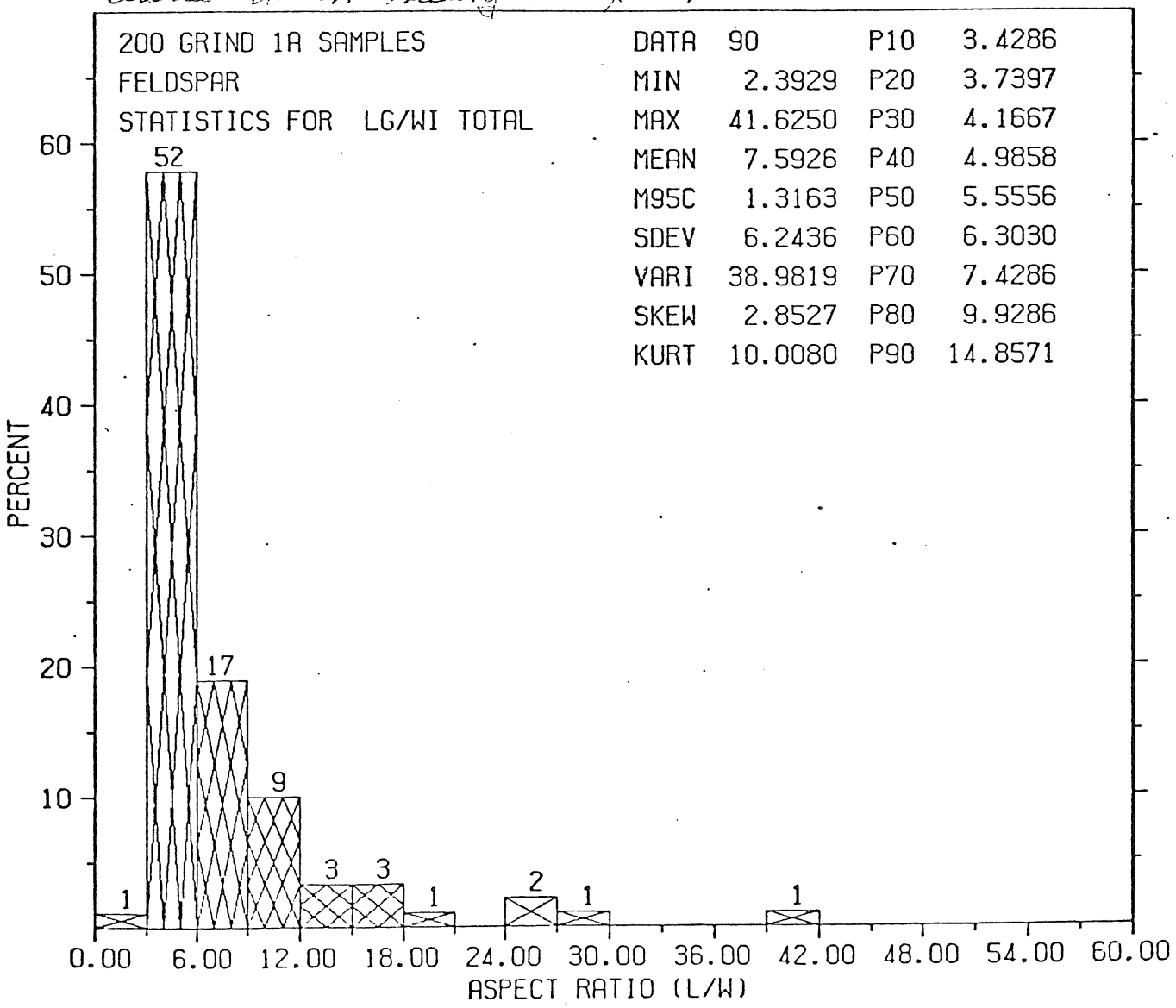

Figure 11

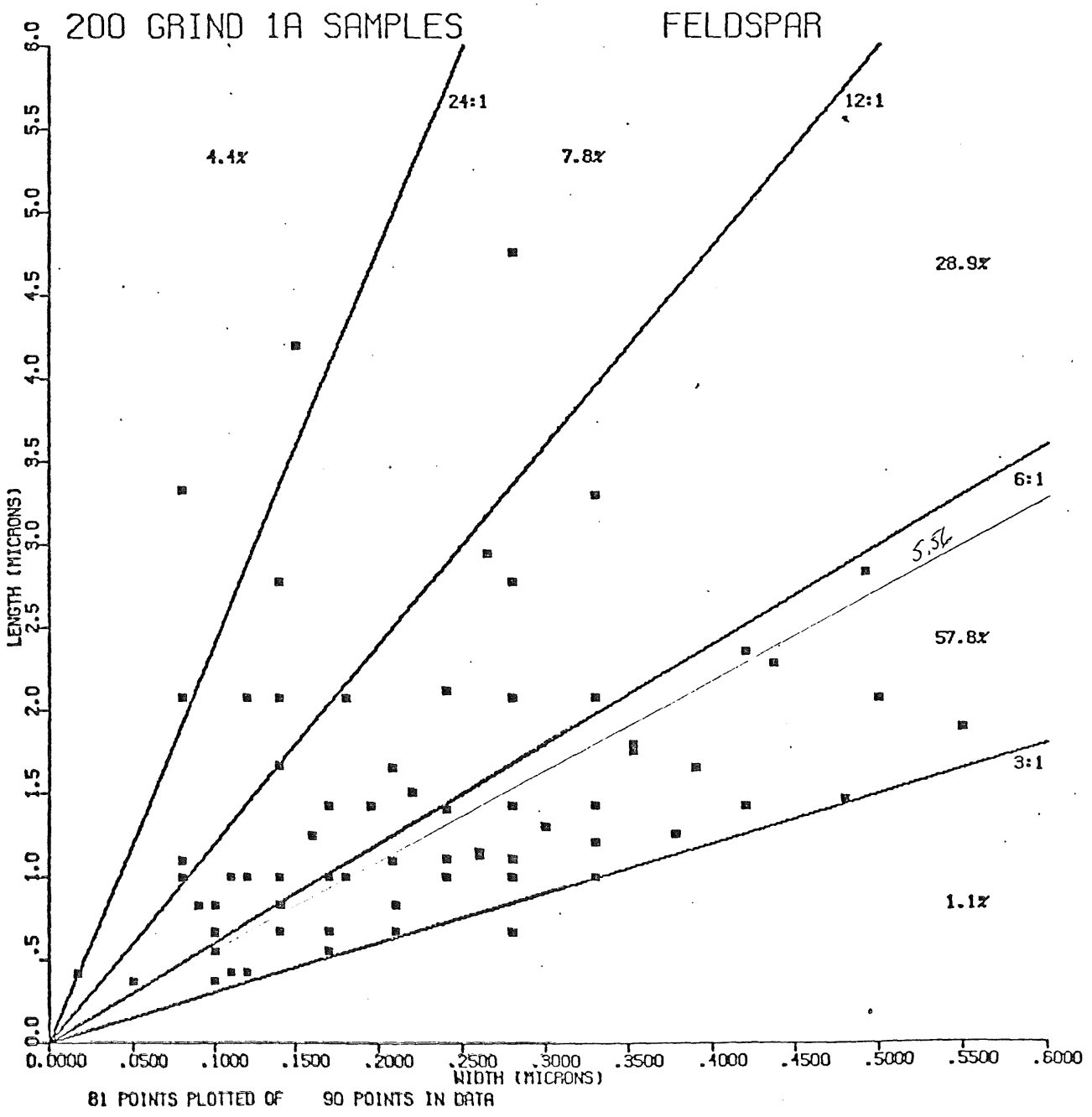

Figure 11: Plot of length versus width for measured plagioclase laths in Tailing samples, 200 mesh grind.

Figure 12

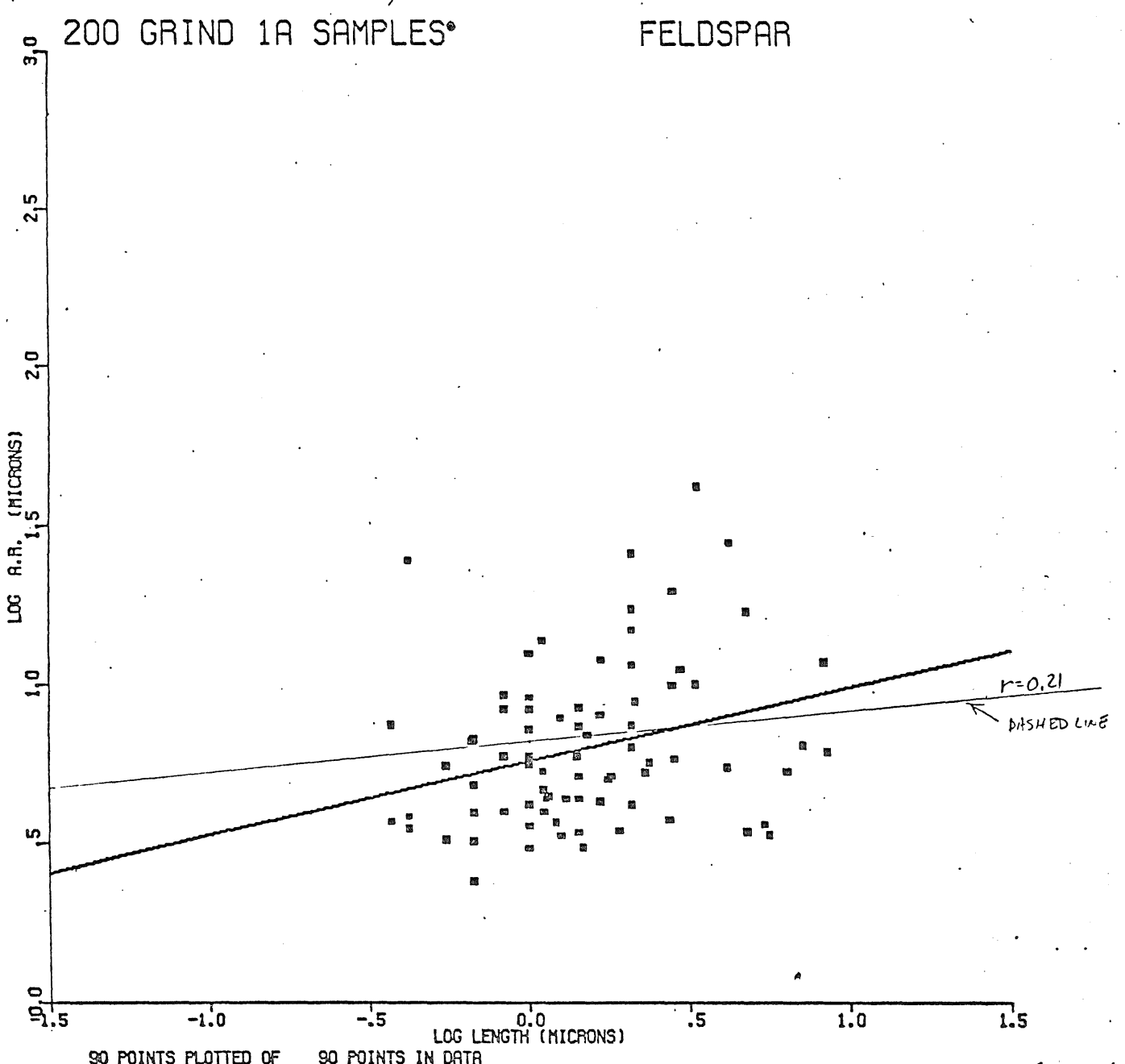

SLOPE	=	.2326 ←	.0841
INTERCEPT	=	.7556 ←	.0290
ROOT MEAN SQ ERROR	=	.2428	
REGRESSION COEF.	=	.2827	
UNCORRELATED PROB.	=	.694335E-02	

Figure 12: log-log plot of aspect ratio versus length for 90 plagioclase fibers from 9 samples (200 mesh grind tailing).

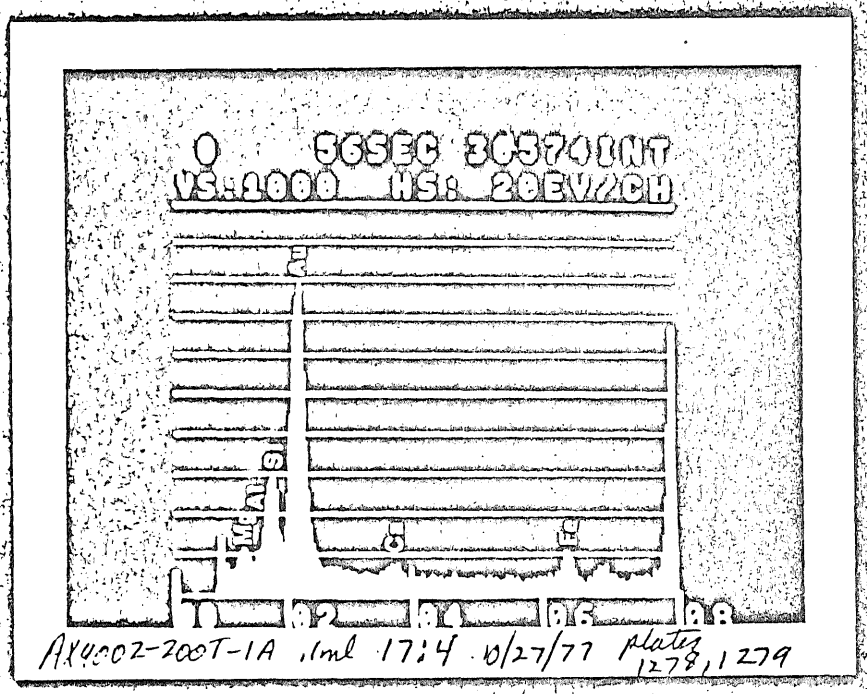

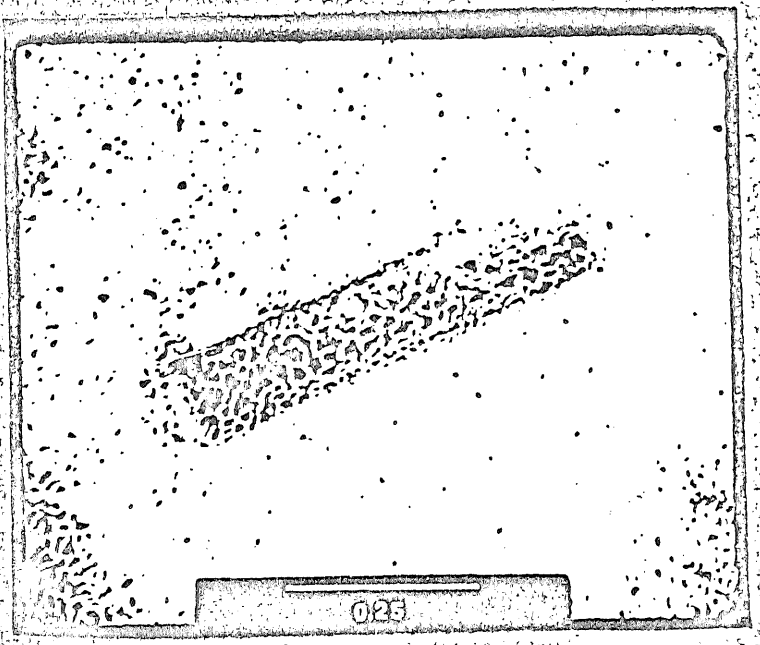

HORNBLENDE

Figure 13

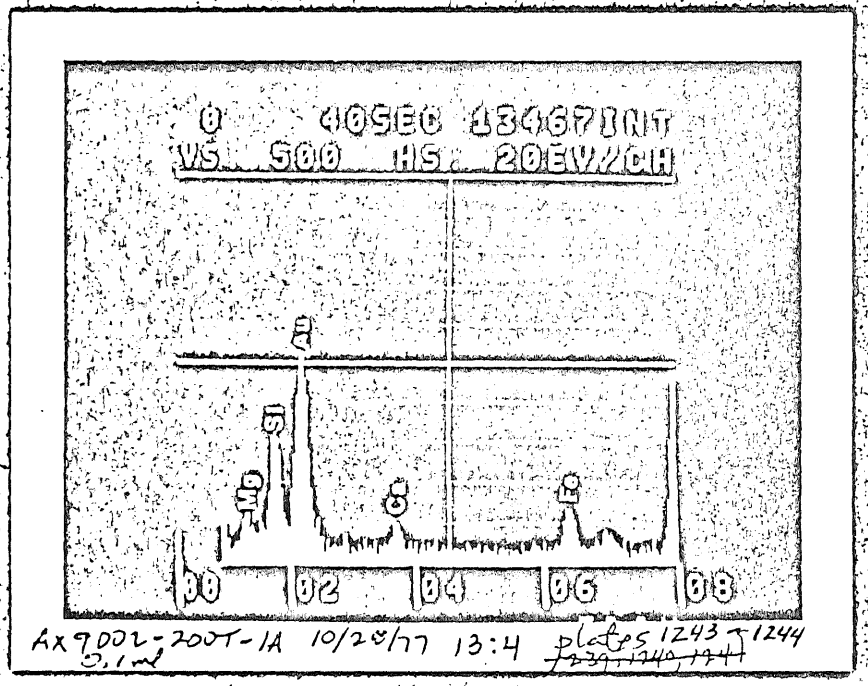

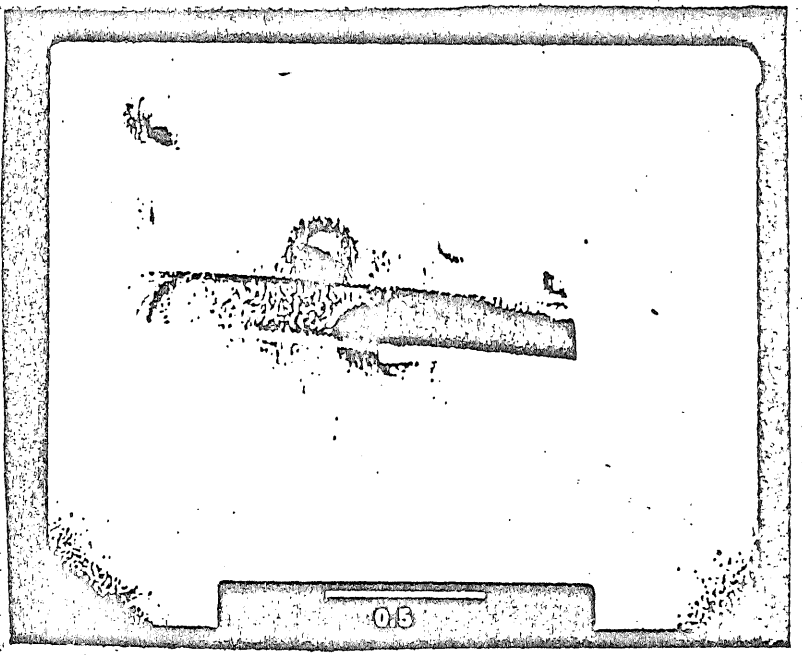

ACTINOLITE

Figure 14

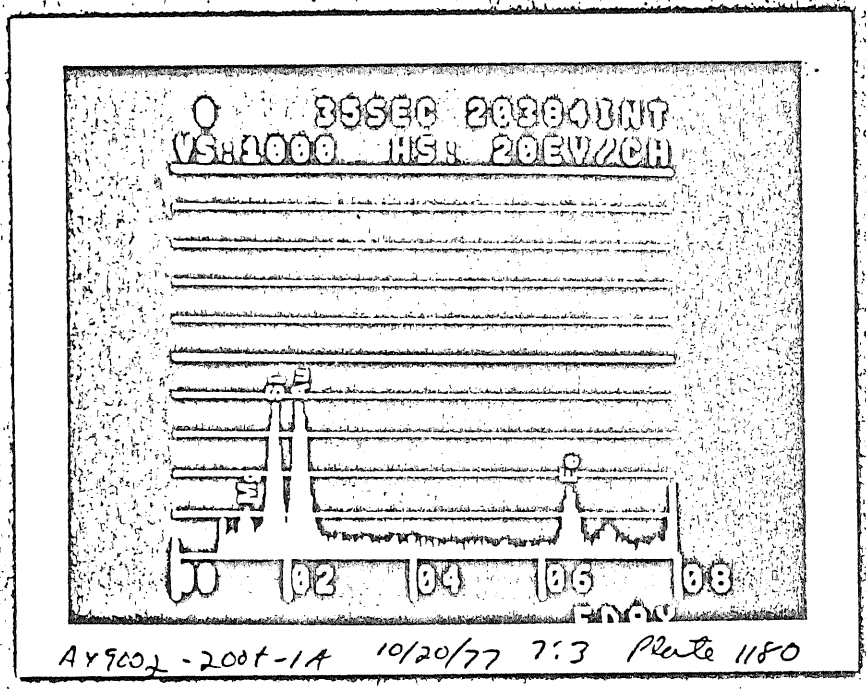

AY902-200f-1A 10/20/77 7:3 Plate 1180

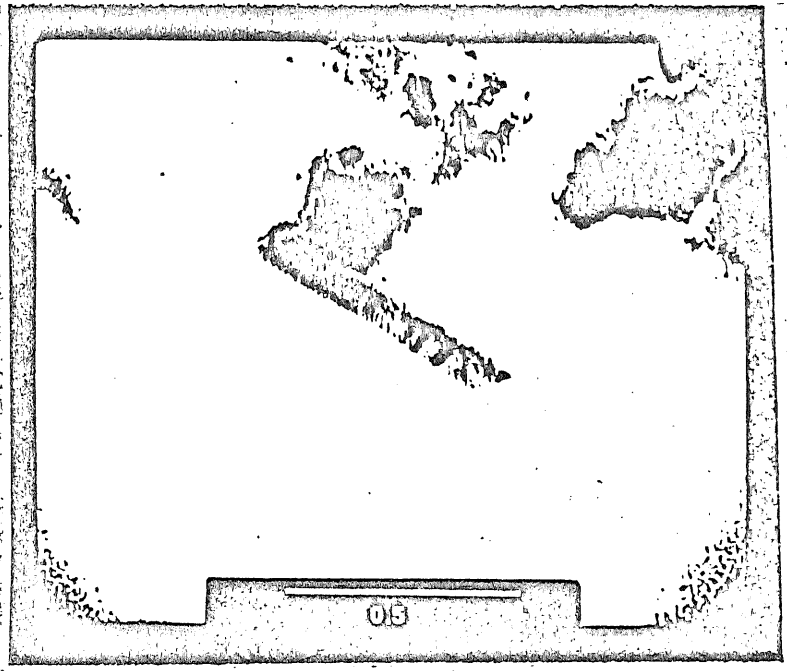

CUMMINGTONITE

Figure 15

Figure 16

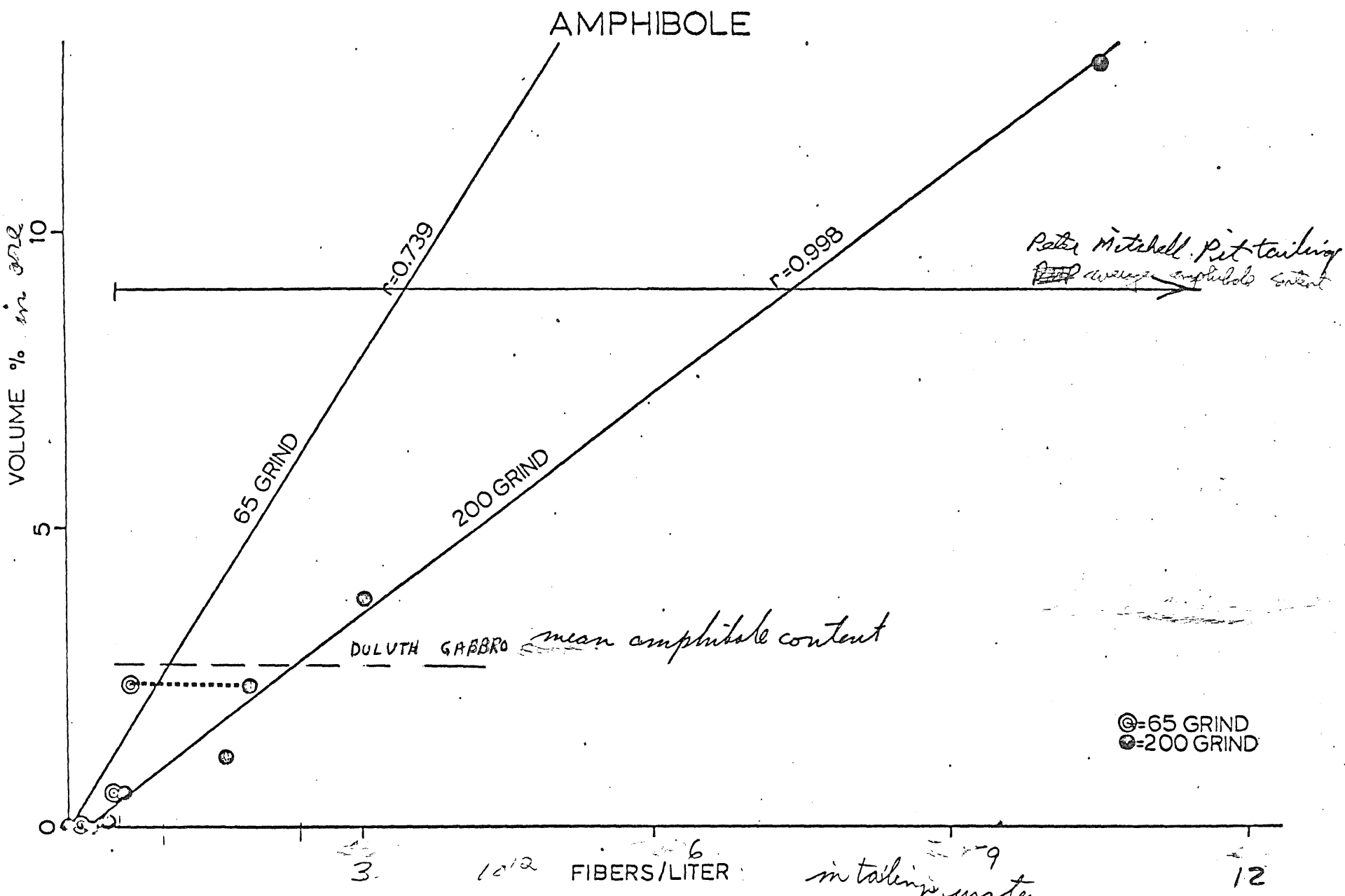

Figure 16: Plot of fibers/liter versus volume % of amphibole in signal ash, for tailing water samples.

Figure 17

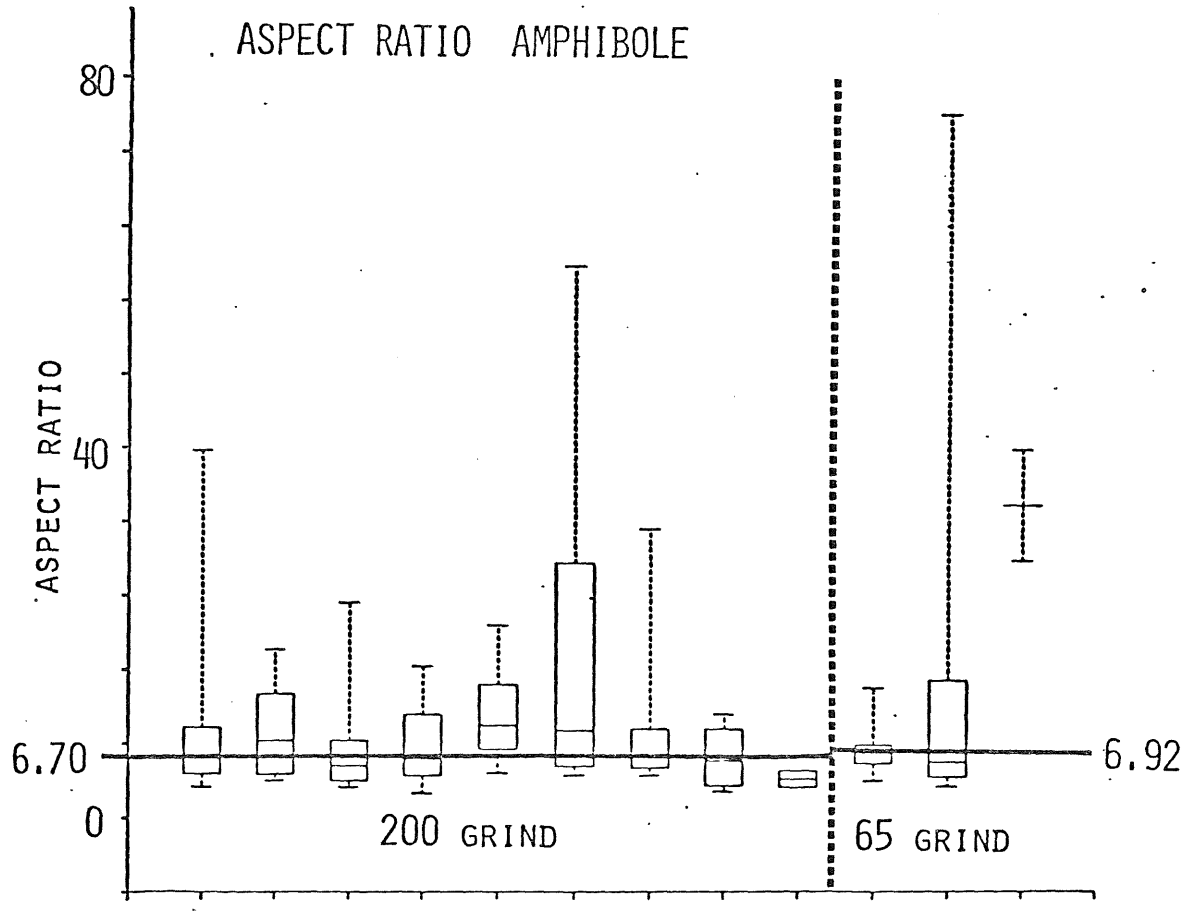

Figure 17: Box plots of aspect ratios for various tailing samples - amphibole only.

Figure 18

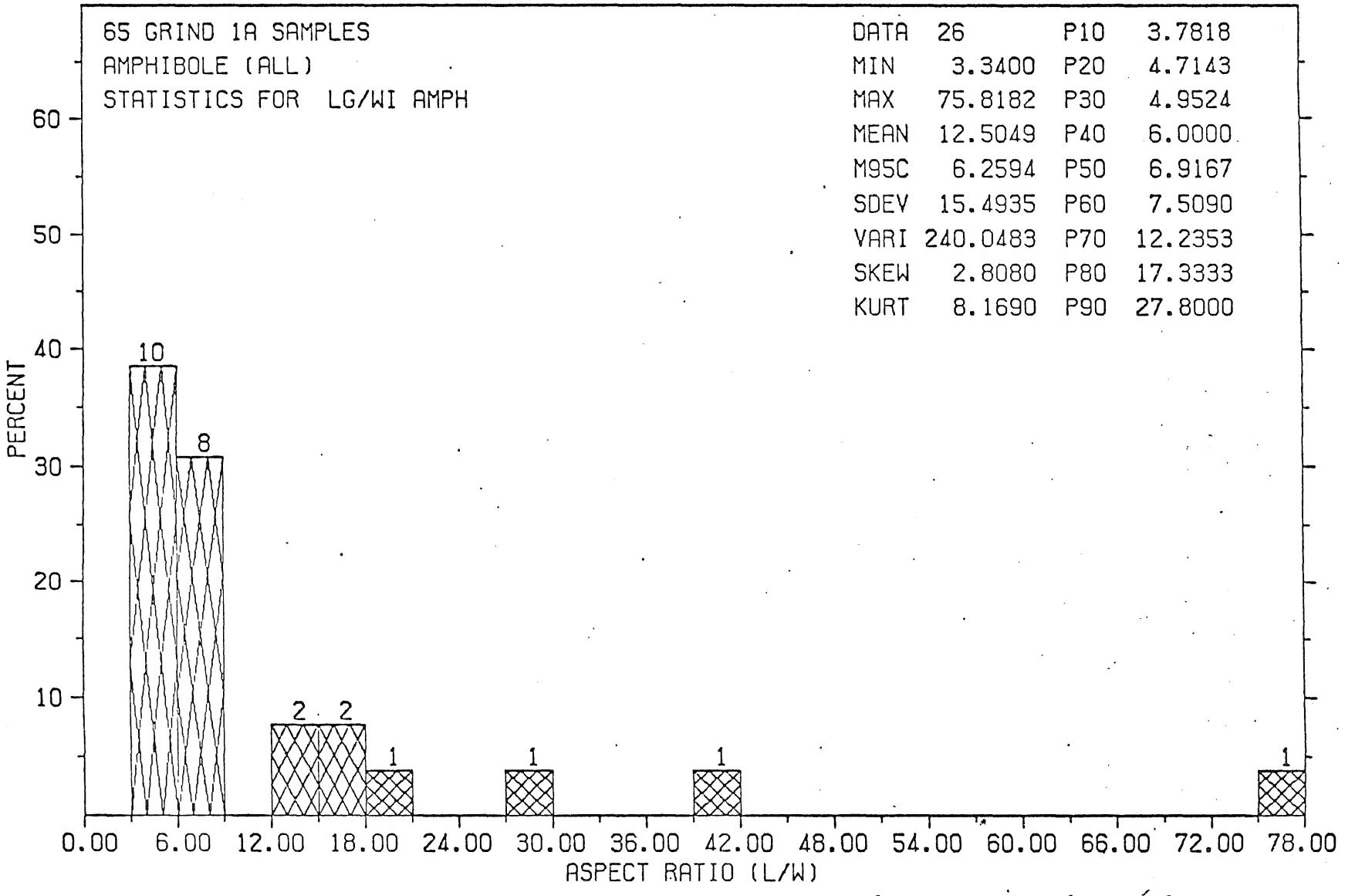

Figure 18 : Distribution of aspect ratios for amphibole fibers measured in 65 mesh grind taling samples.

Figure 19.

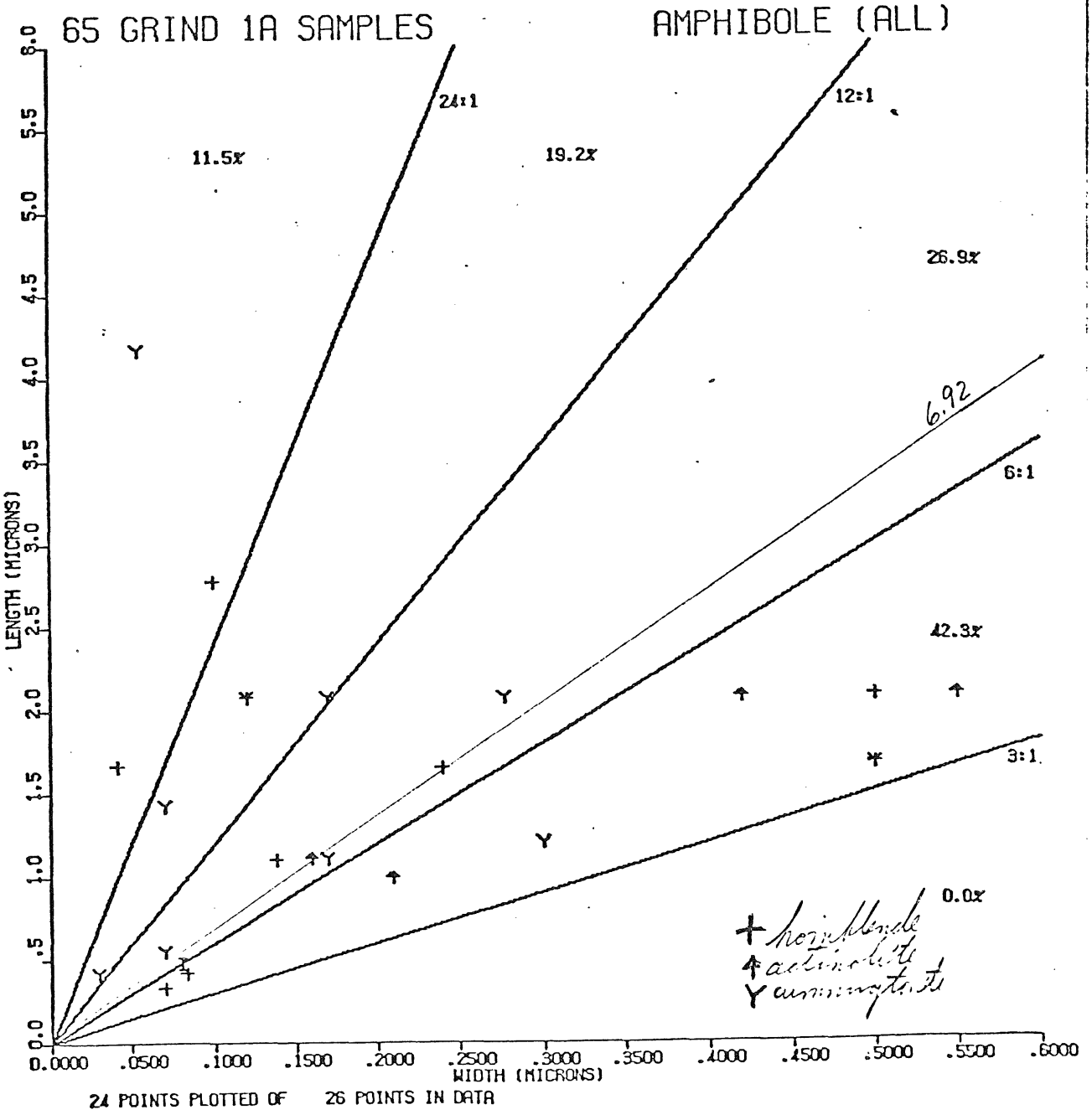

Figure 19: Plot of length versus width for amphibole fibers measured in 65 mesh grind tailing samples.

Figure 20

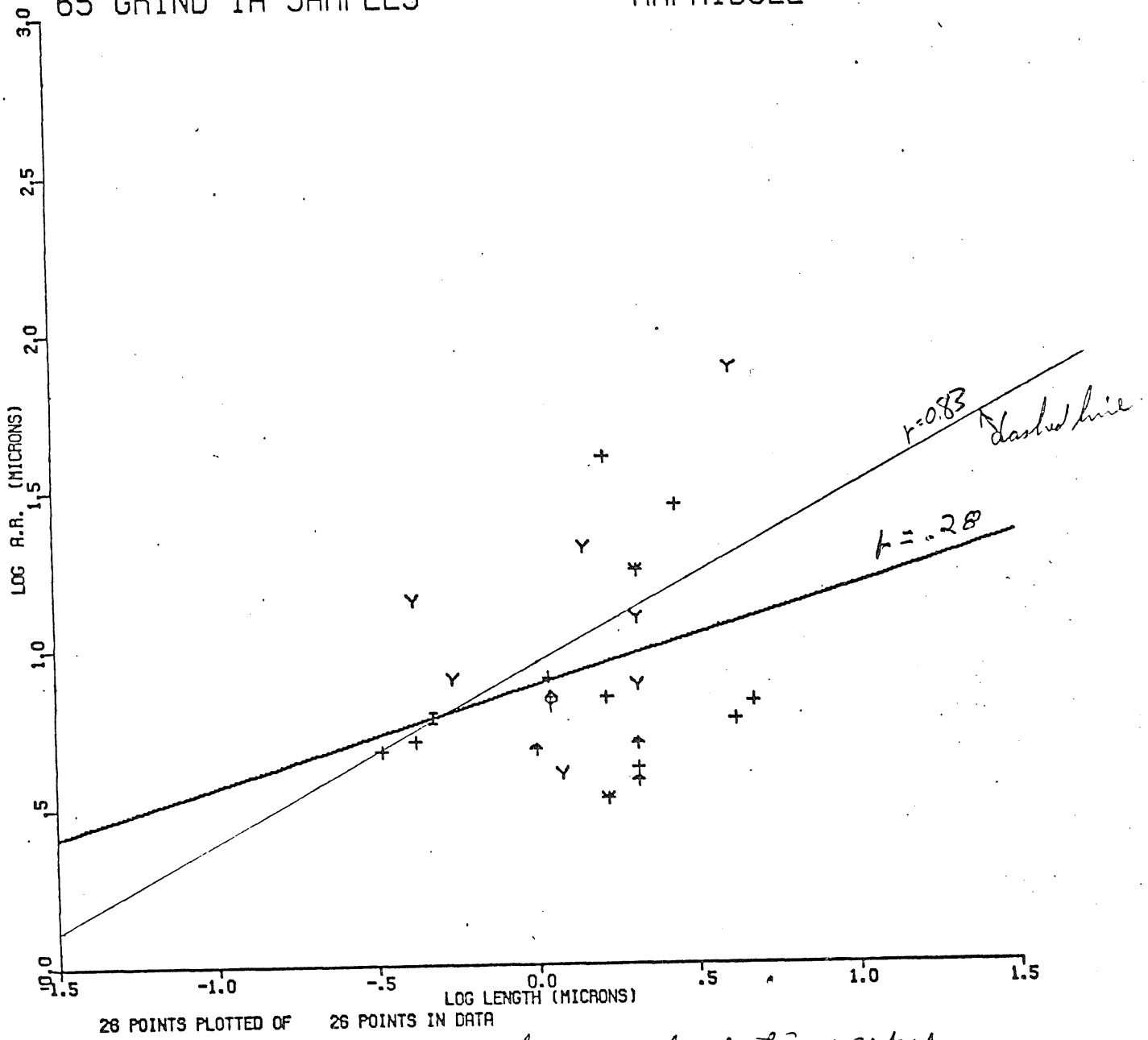

SLOPE	=	.9132 ←	.2180
INTERCEPT	=	.8777 ←	.0747
ROOT MEAN SQ ERROR	=	.3398	
REGRESSION COEF.	=	.2815	

Figure 20: Log-log plot of aspect ratio versus length for amphibole fibers measured in 65 mesh grind tailing samples.

Figure 21
Distribution of aspect ratio for amphibole fibers measured in 200 mesh grind tailing samples.

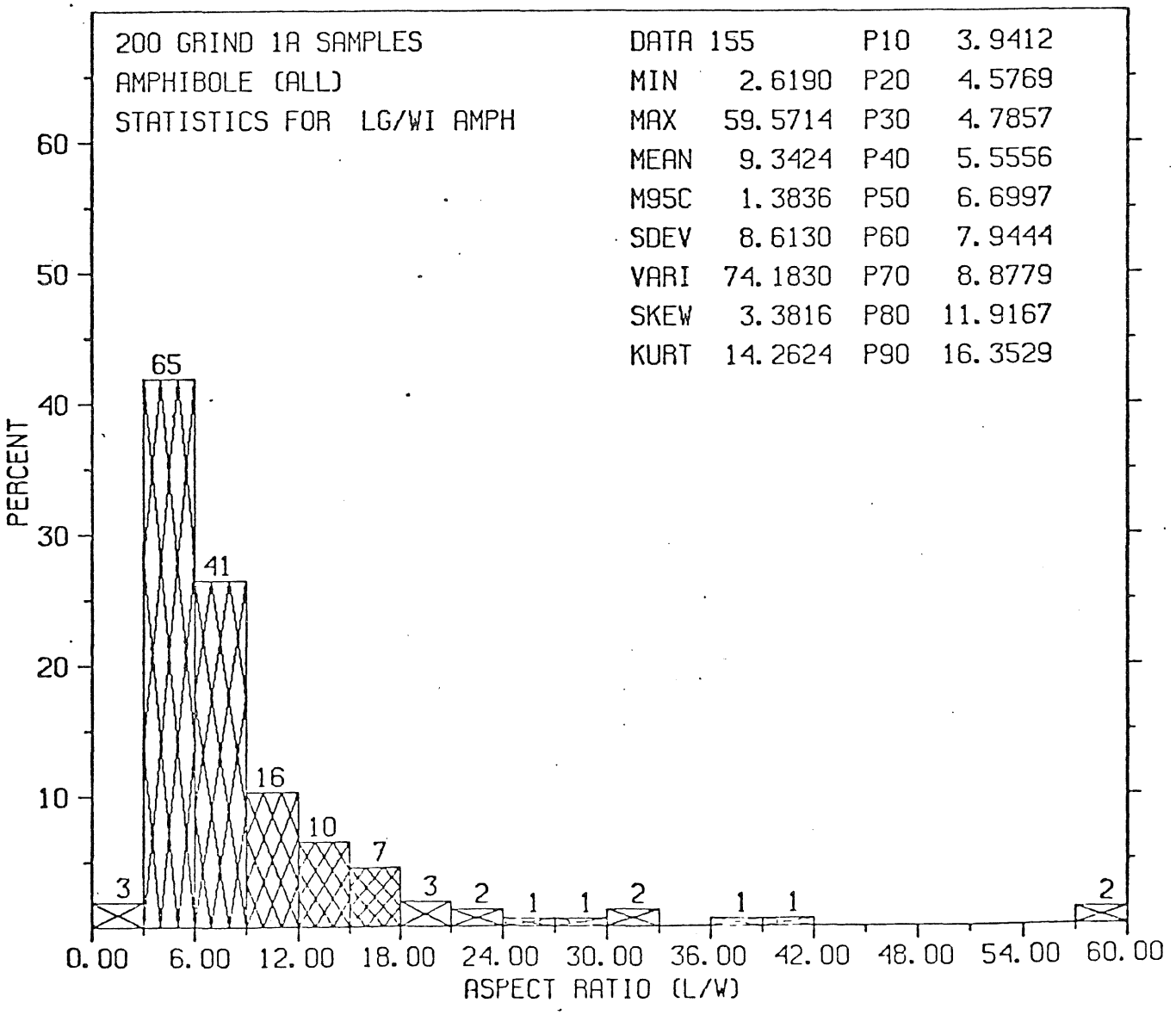

Figure 22

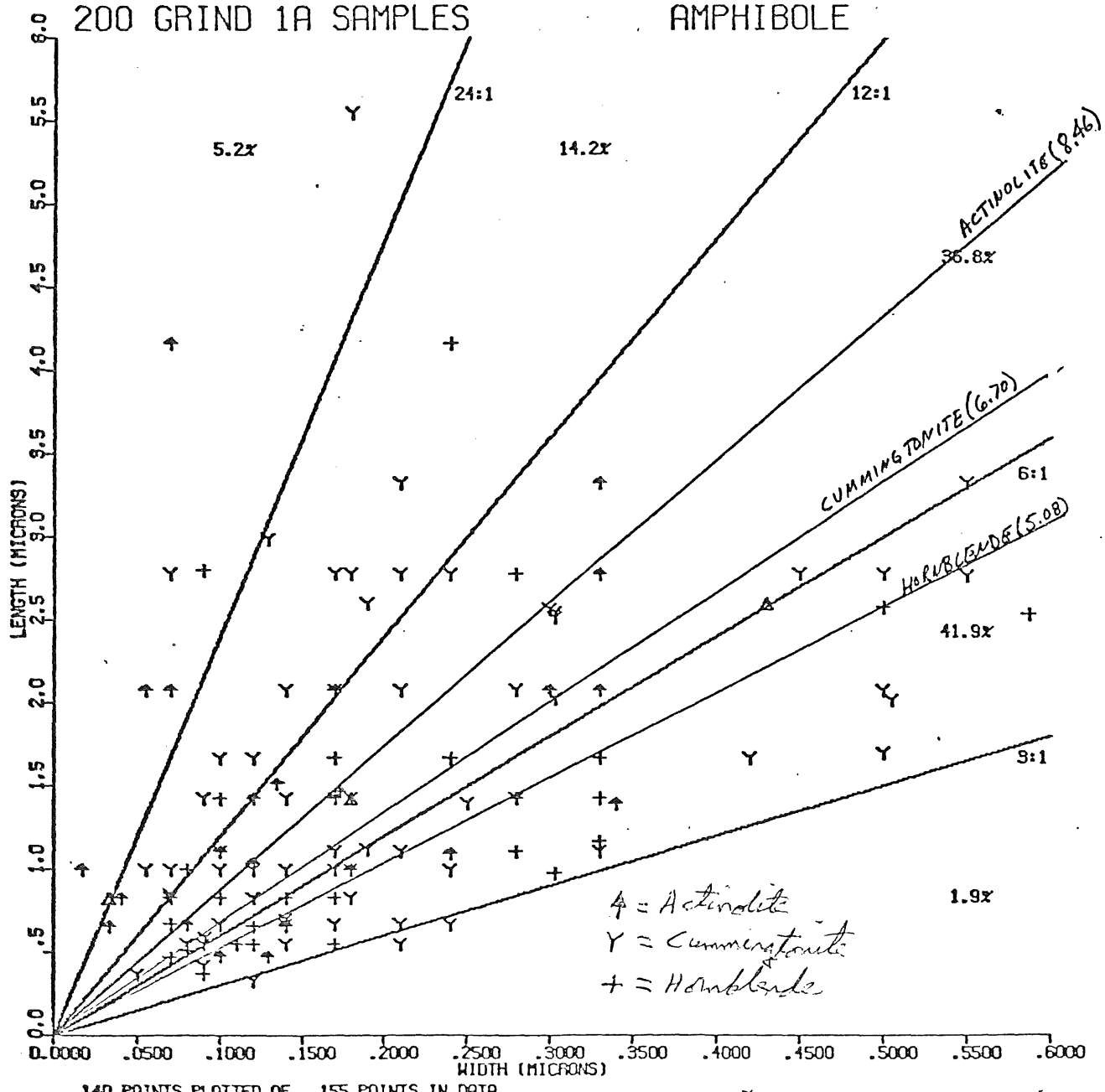

Figure 22: plot of length versus width for amphibole fibers measured in 200 mesh grind tailing samples.

Figure 23

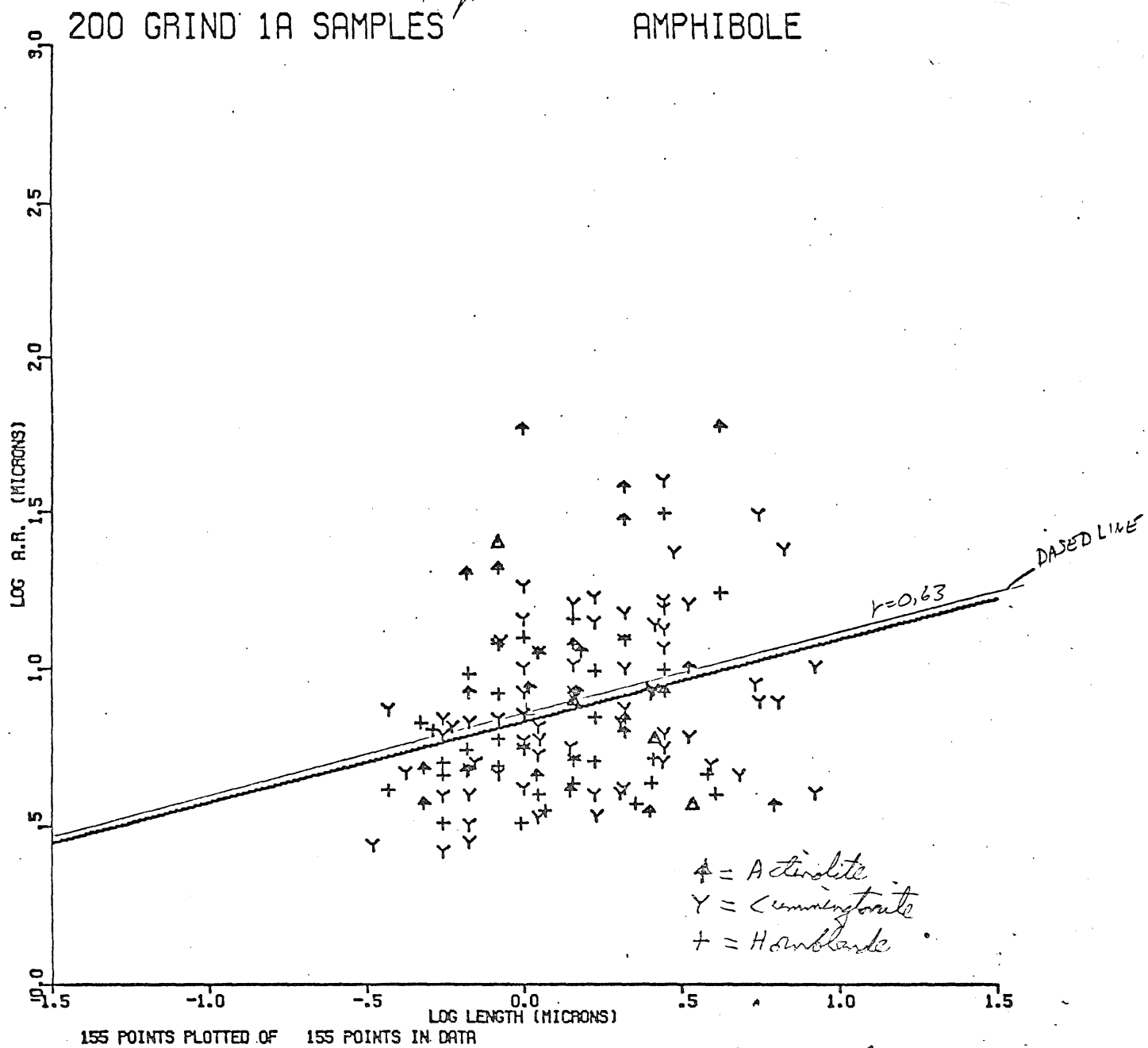

SLOPE	=	.2578 ±	.0678
INTERCEPT	=	.8919 ±	.0230
ROOT MEAN SQ ERROR	=	.2579	
REGRESSION COEF.	=	.2939	

Figure 23 : log-log plot of length versus width for 155 amphibole fibers in 200 mesh grind taking samples.

Figure 24

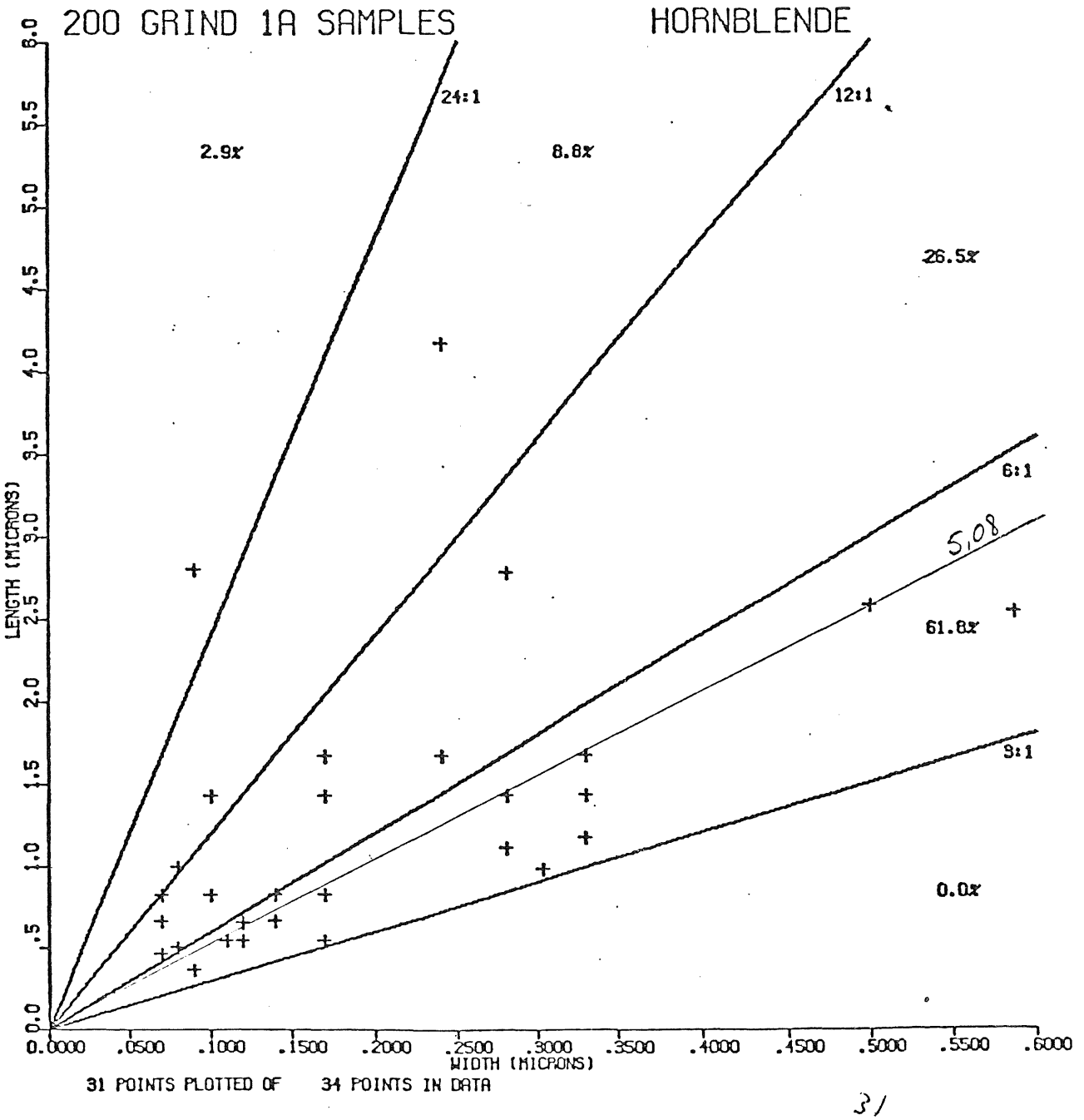

Figure 24: Plot of length versus width for 31 hornblende fibers in 200 mesh grind tailing samples.

Figure 25

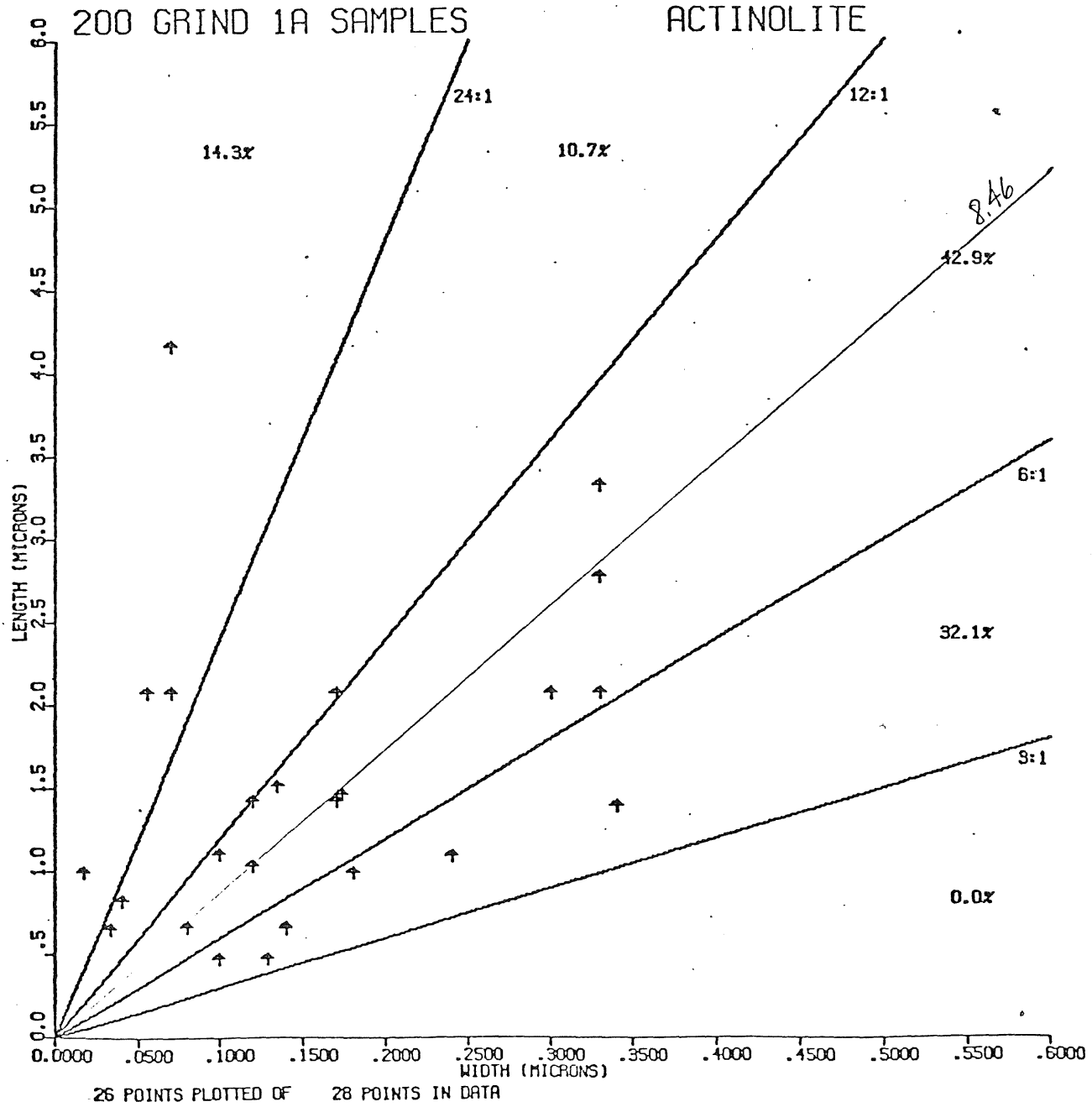

Figure 25: Plot of length versus width for 28 actinolite fibers in 200 mesh grind Tailing Samples.

Figure 26

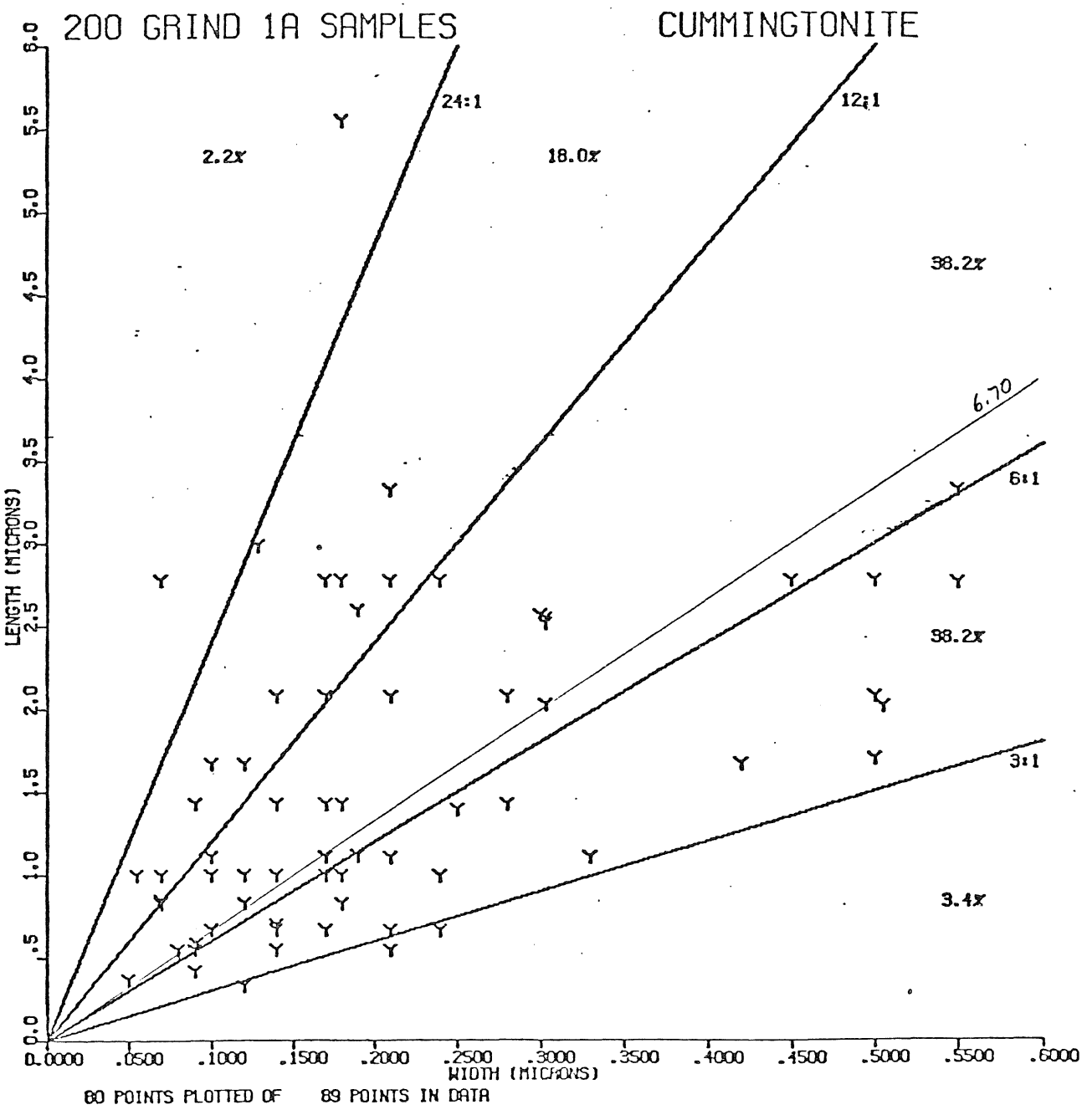

Figure 26: Plot of Length versus width for 89 cummingtonite fibers in 200 mesh grind tailing samples.

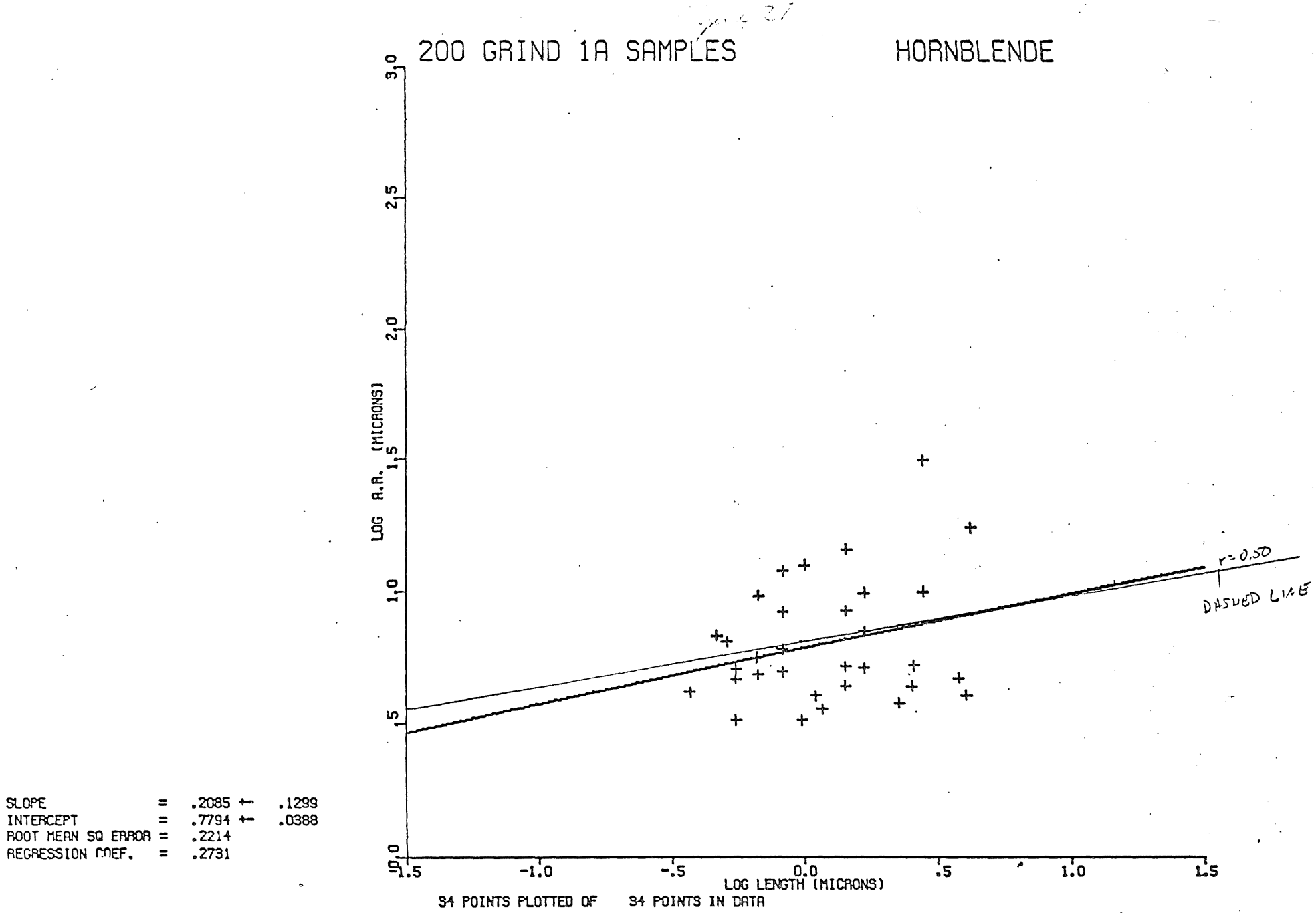

Figure 27: Log-log plot of aspect ratio versus length for 34 Hornblende fibers in 200 mesh grind taling samples.

Figure 28

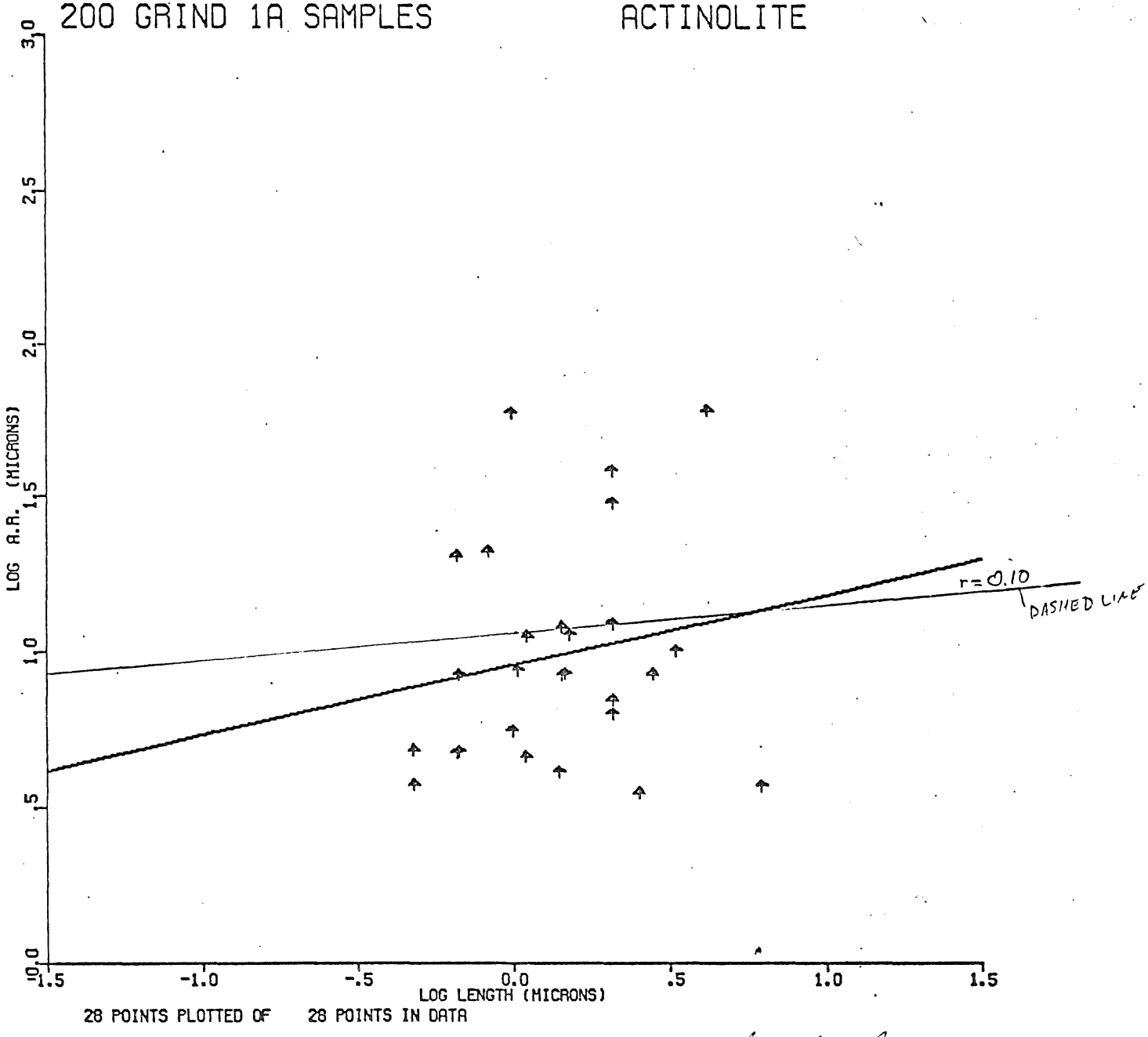

SLOPE	=	.2240 ←	.2425
INTERCEPT	=	.9530 ←	.0745
ROOT MEAN SQ ERROR	=	.3487	
REGRESSION COEF.	=	.1783	

Figure 28: Log-log plot of aspect ratio versus length for 28 actinolite fibers in 200 mesh grind tailing samples.

Figure 29

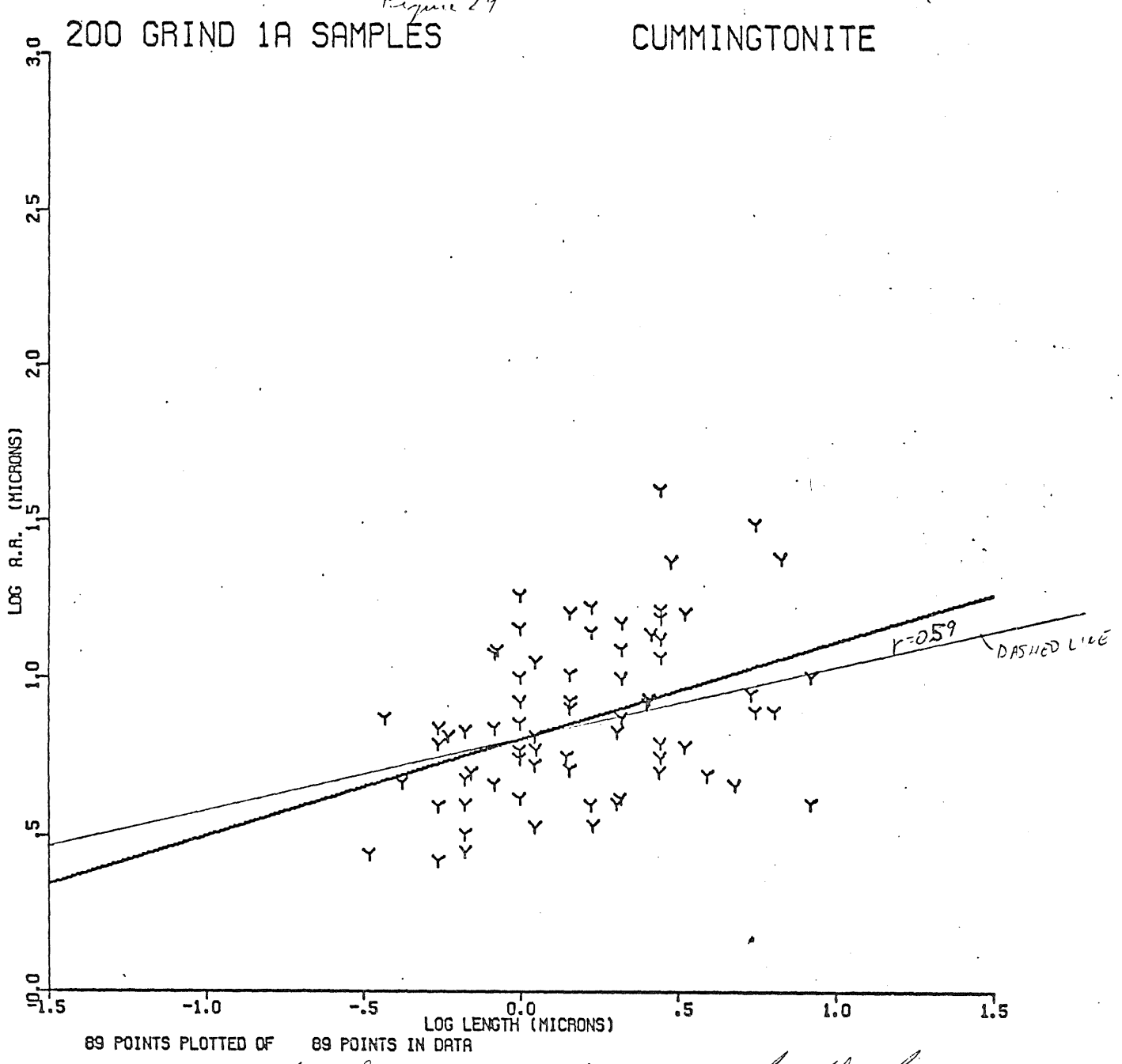

SLOPE	=	.3069 ±	.0752
INTERCEPT	=	.8061 ±	.0272
ROOT MEAN SQ ERROR	=	.2244	
REGRESSION COEF.	=	.4008	

Figure 29: Log-log plot of aspect ratio versus length for 89 cummingtonite fibers in 200 mesh grind talc samples.

Figure 30

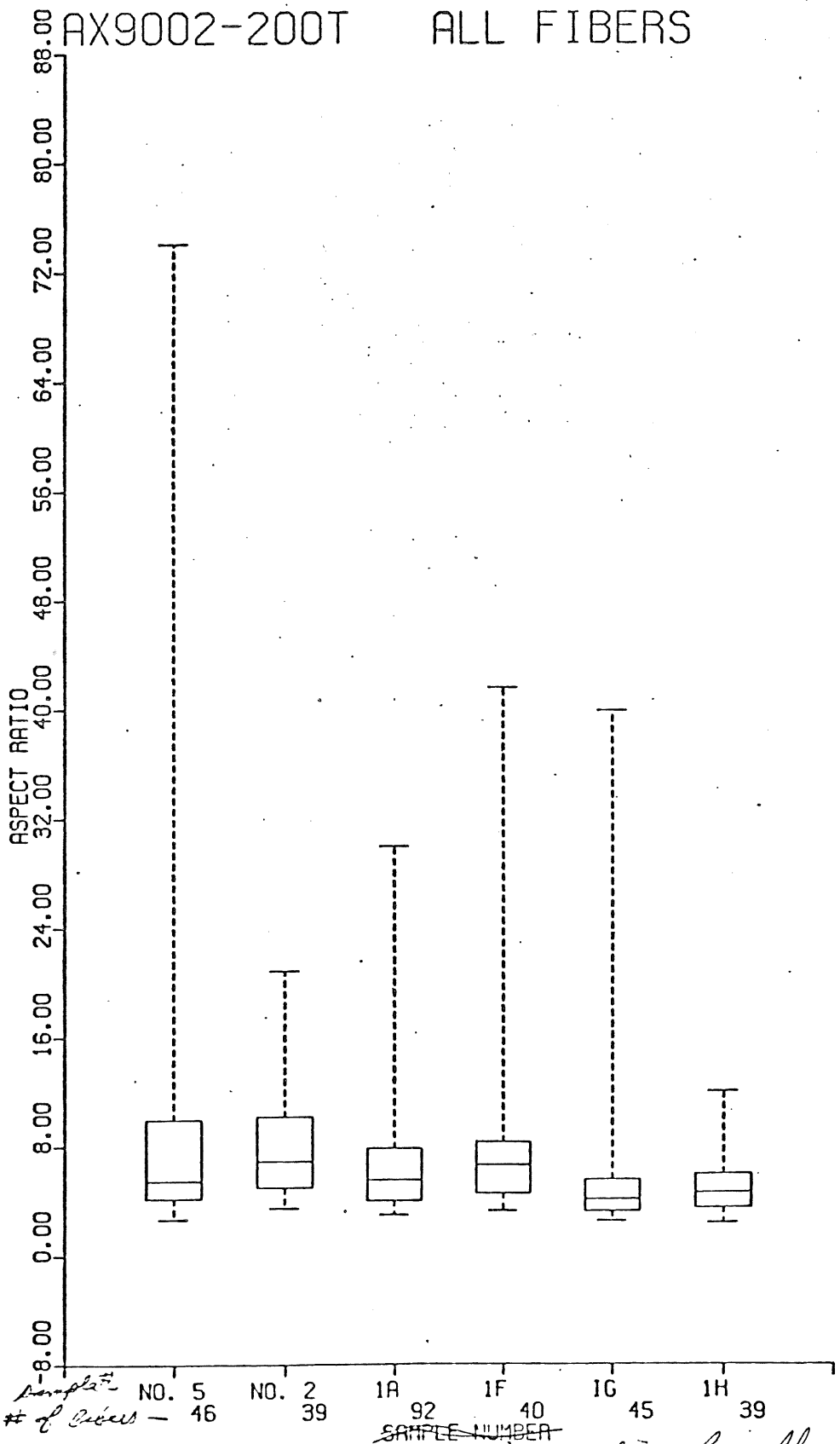

Figure 30: Box plots of aspect ratios for all fibers measured in a 200 mesh grind tailing sample; time sequence study.

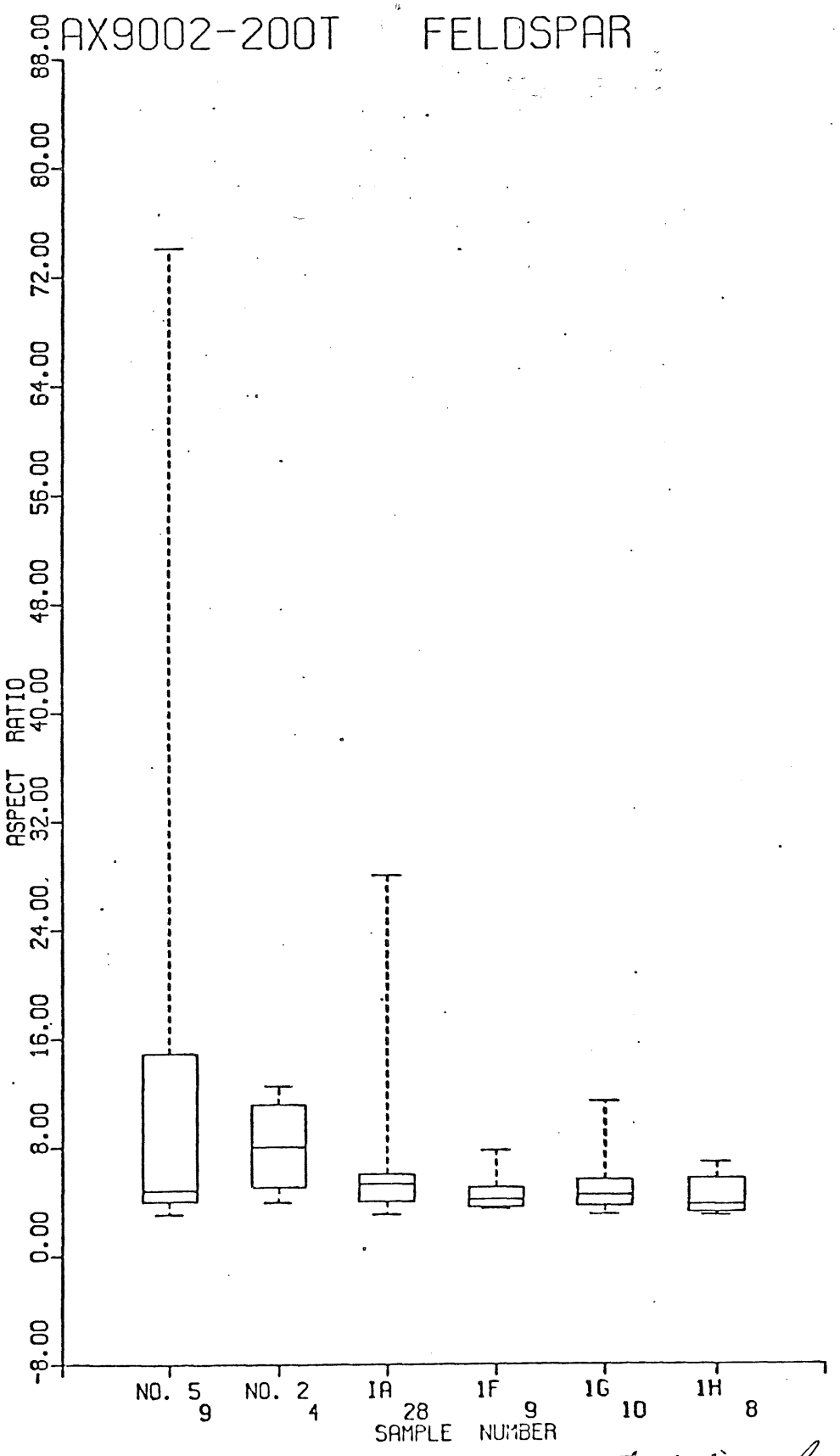

Figure 31: Box plots of aspect ratio of feldspar (plagioclase) fibers measured in a 200 mesh grind tailing sample; Libby Sequence Study.

Figure 32

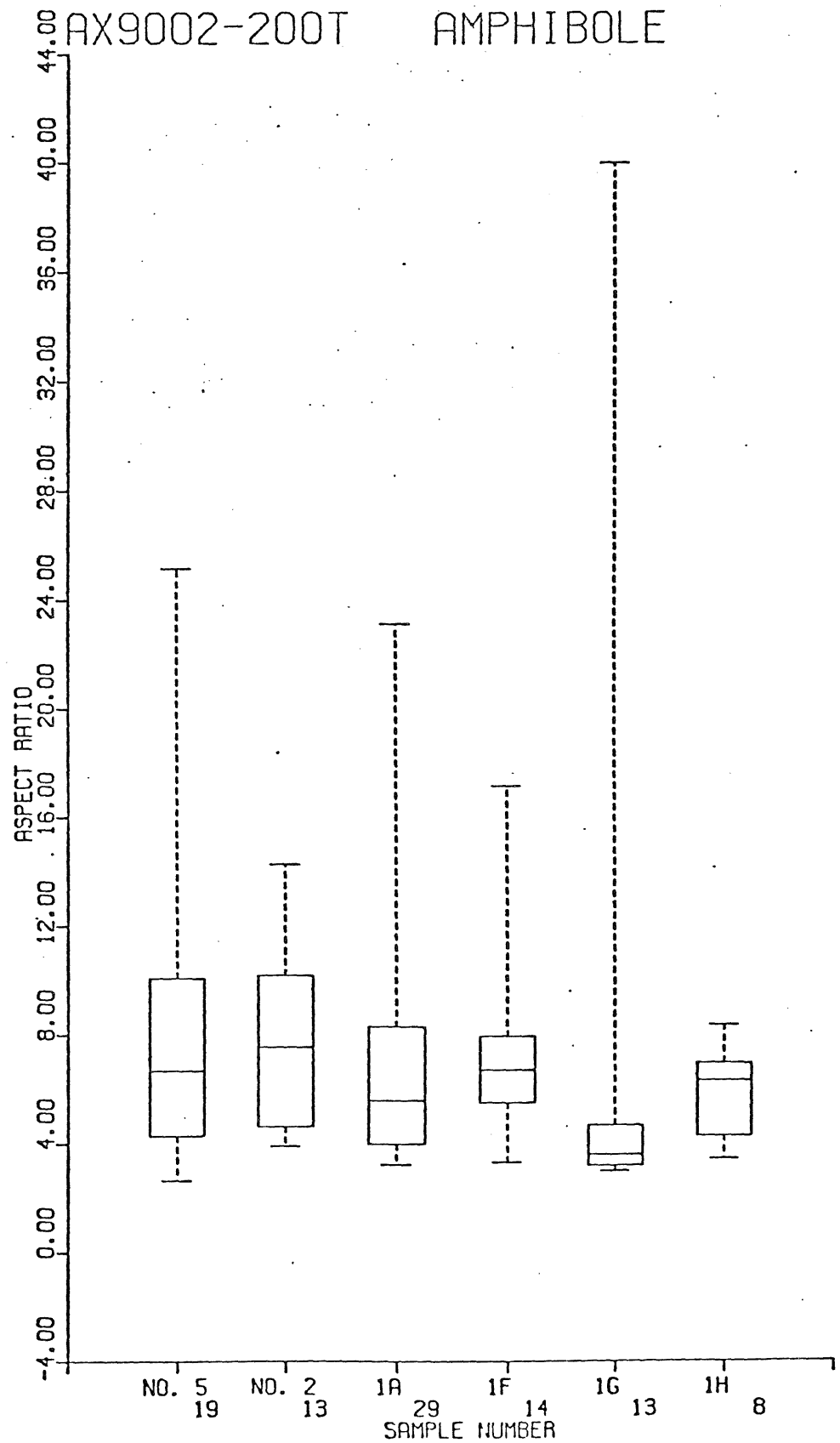

Figure 32: Box plots of aspect ratio for amphibole fibers measured in a 200 mesh grind tailing sample; time sequence study.

Figure 33

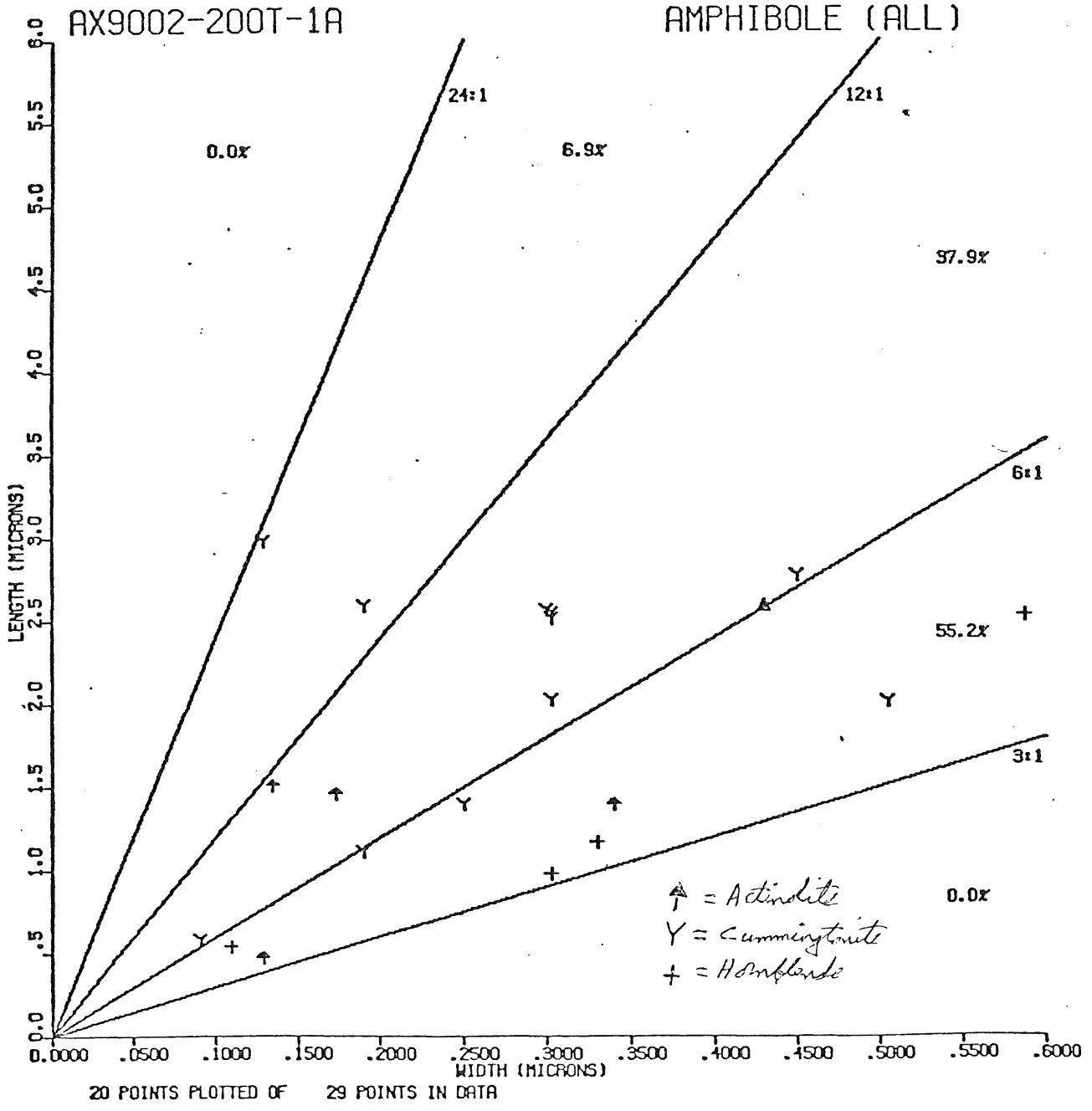

Figure 33: plot of length versus width for all measured amphibole fibers in a 200 mesh grind tailing sample.

Figure 34

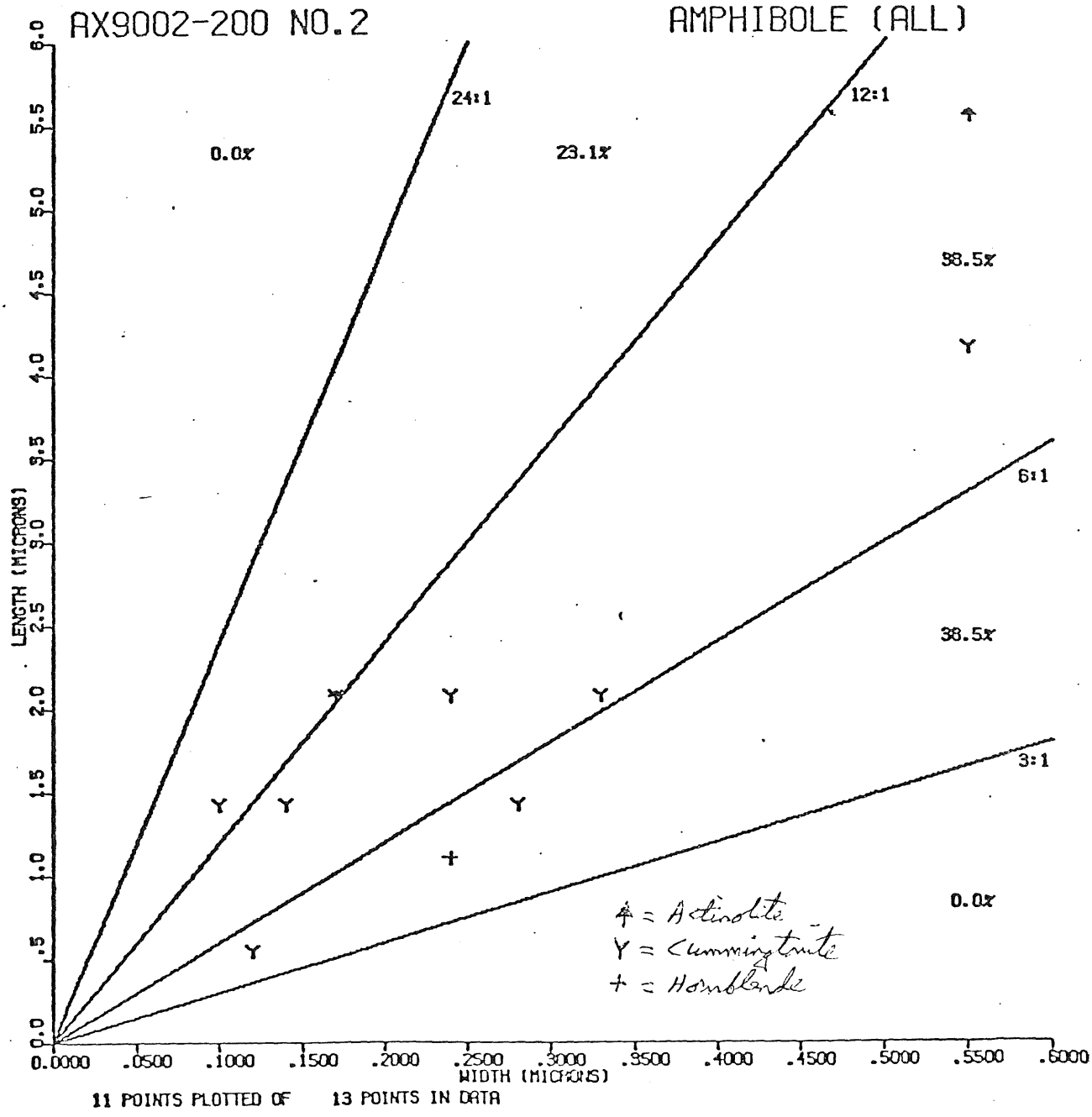

Figure 34: Plot of length versus width for all measured amphibole fibers in a 200 mesh grind Libby Sample.

Figure 35

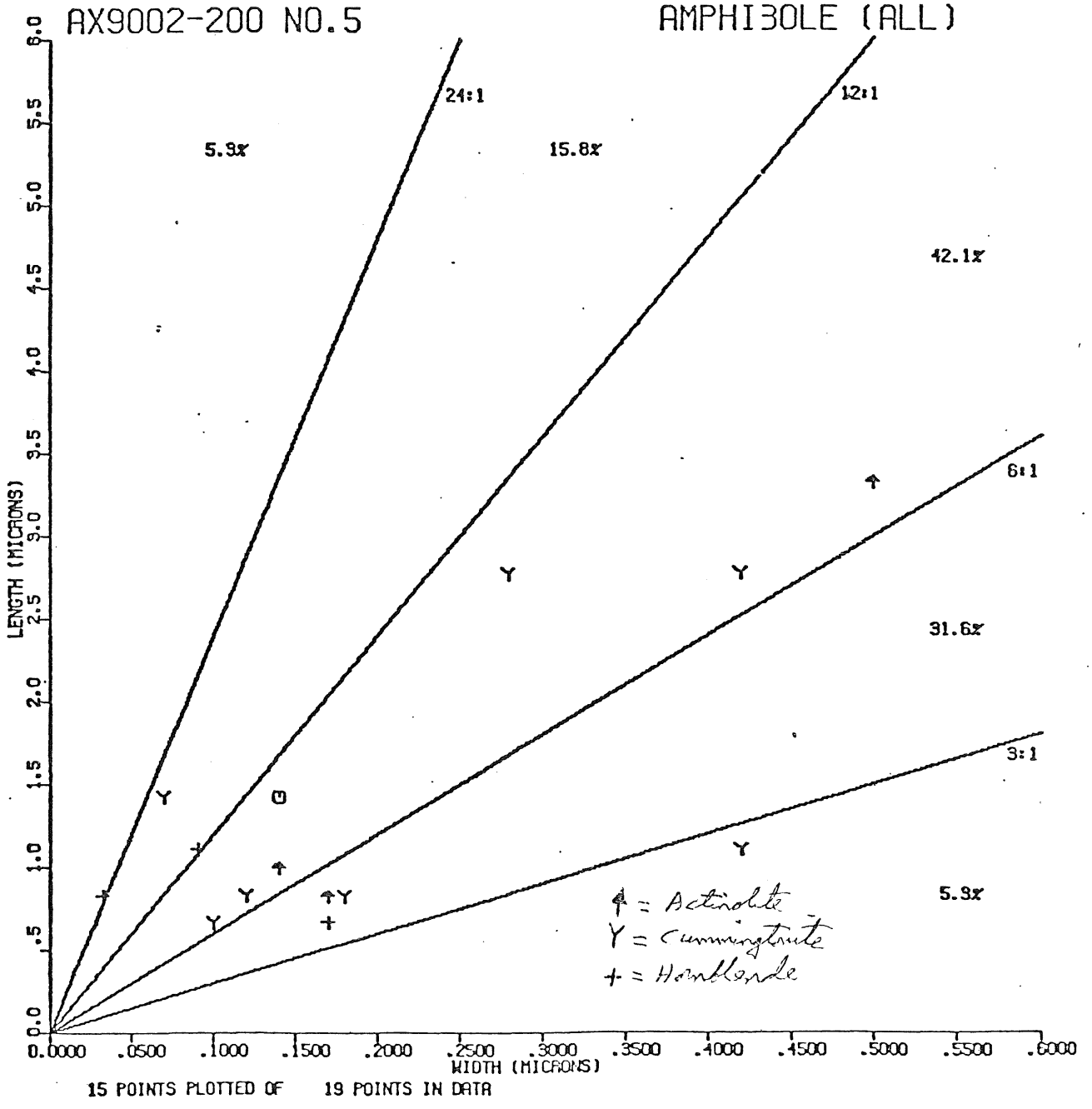

Figure 35: Plot of length versus width for all measured amphibole fibers in a 200 mesh grind tailing sample.

Figure 36

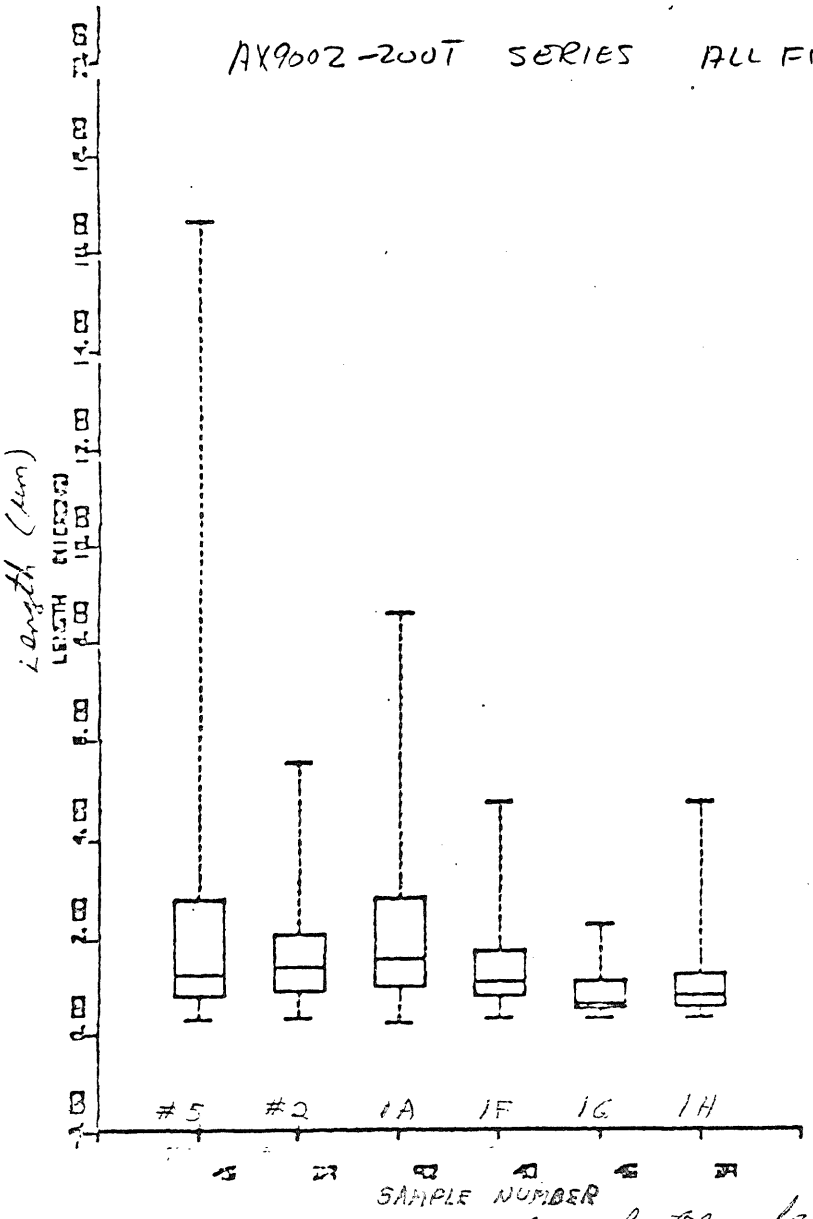

Figure 36: Box plots of the length of all fibers measured in a 200 mesh grind tailing sample; time sequence study.

Figure 37.

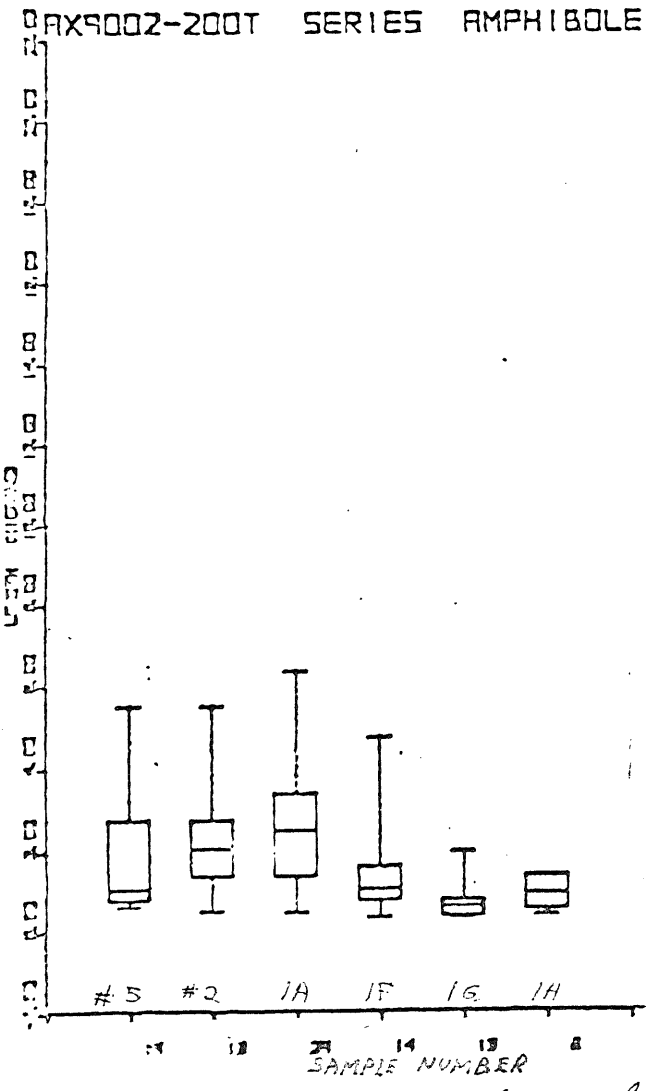

Figure 37 - Box plots of the length of amphibole fibers measured in a 200 mesh grind tailing sample; time sequence study.

Figure 38

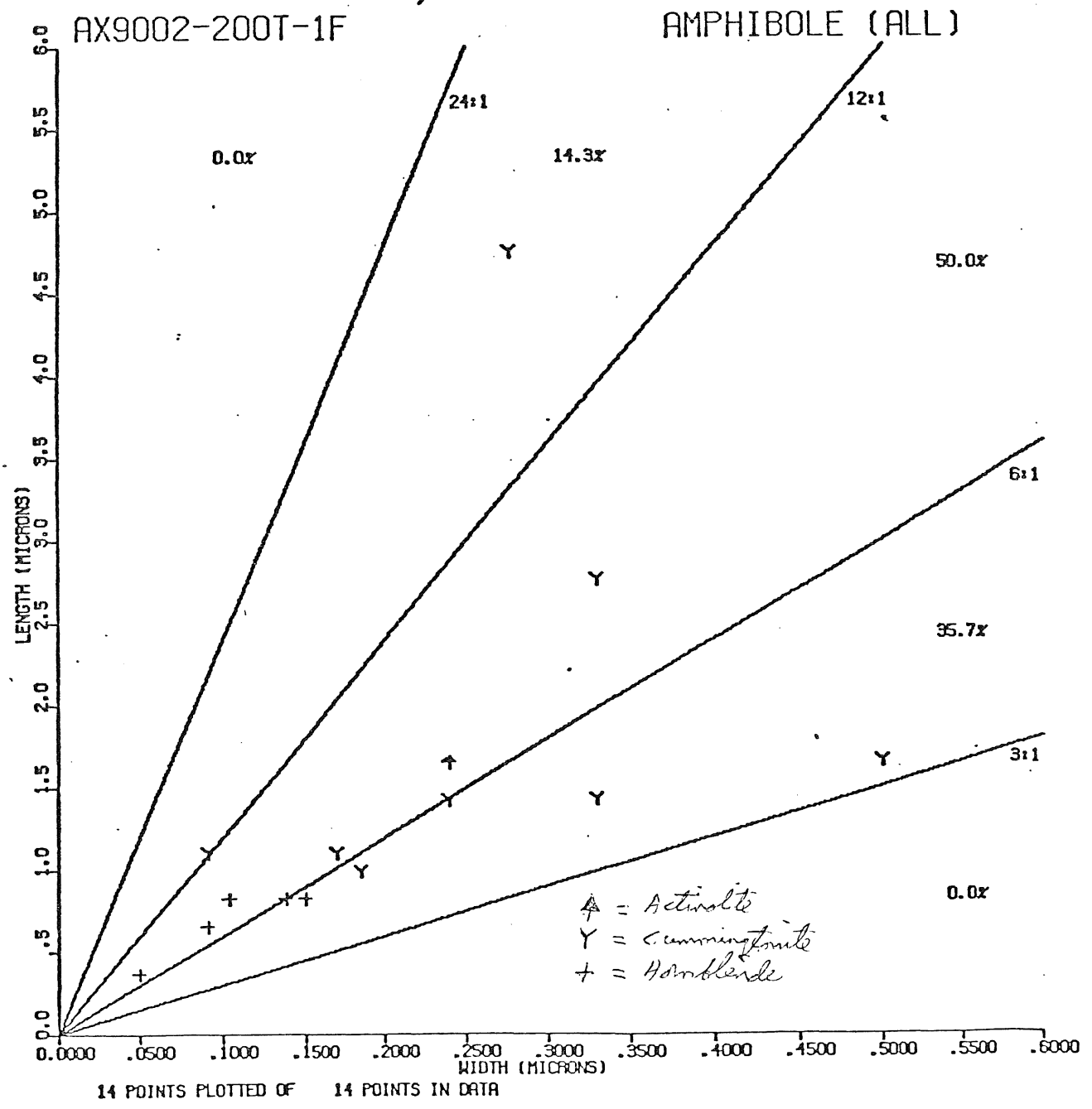

Figure 38: Plot of length versus width for all measured amphibole fibers in a 200 mesh grind Tailing Sample.

Figure 39

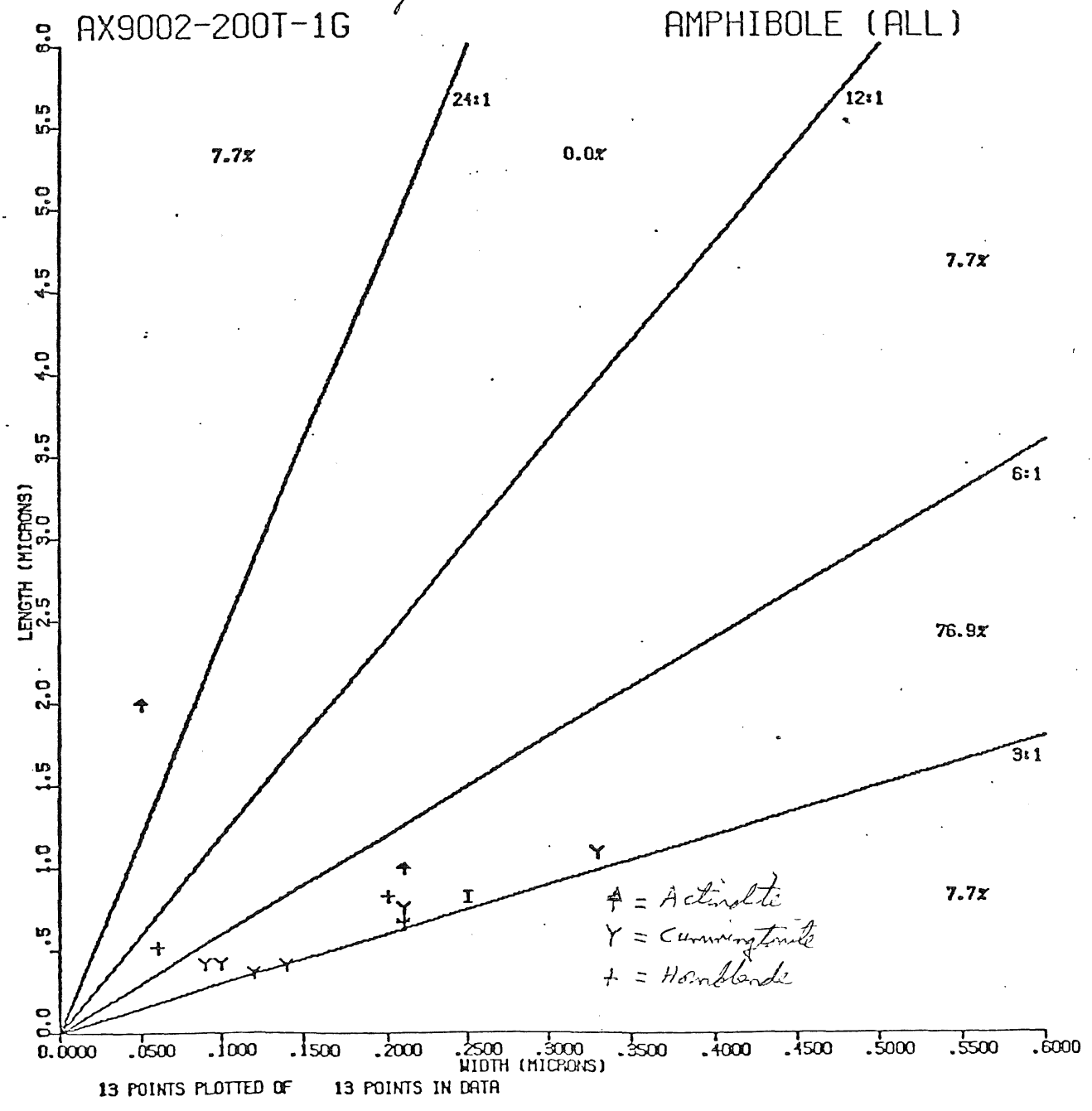

Figure 39: plot of length versus width for all measured amphibole fibers in a 200 mesh grind tailing sample.

Figure 40

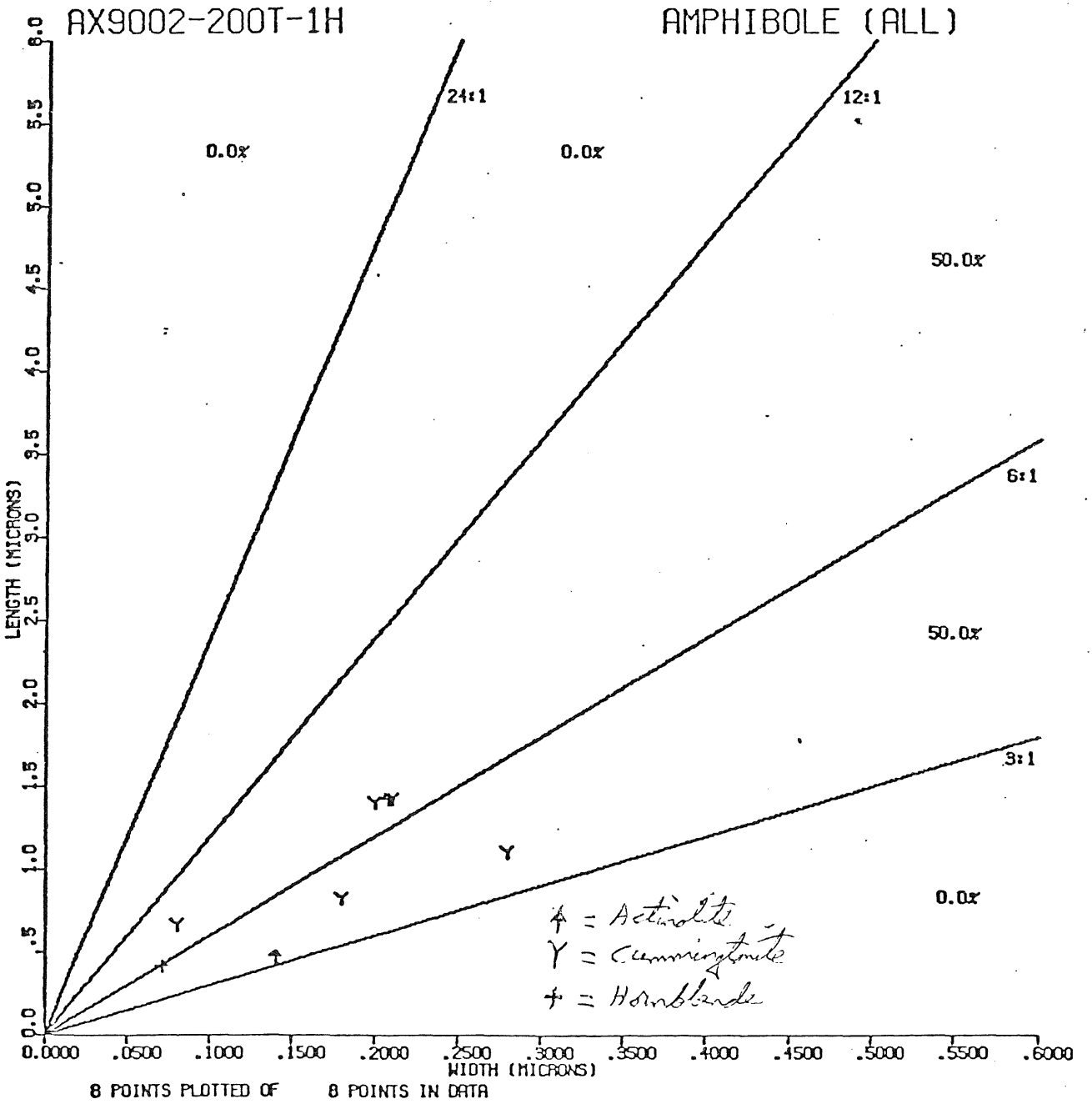

Figure 40: Plot of length versus width for all measured amphibole fibers in a 200 mesh grind tailing sample.

Figure 41
Boxplot of length for AX9002 samples

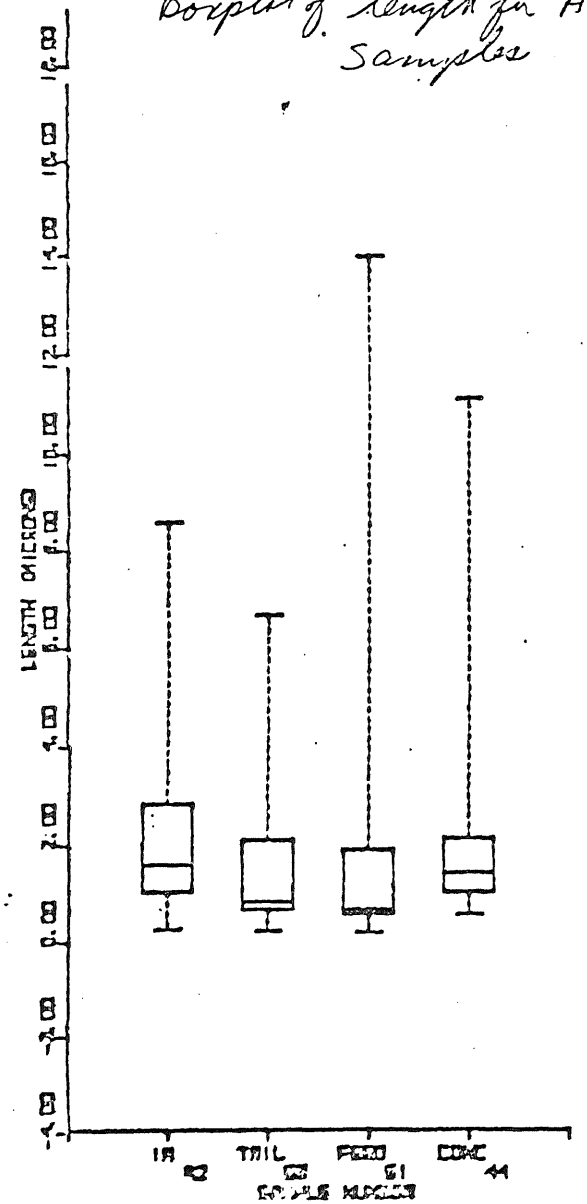

Figure 41: Box plot of lengths of all measured fibers for several samples (feed, concentrate, solid tails, tailing slurry) originating from one rock sample.

Figure 42. Thin sections of Binisk 1F(a) and Duluth Gabbro(b)

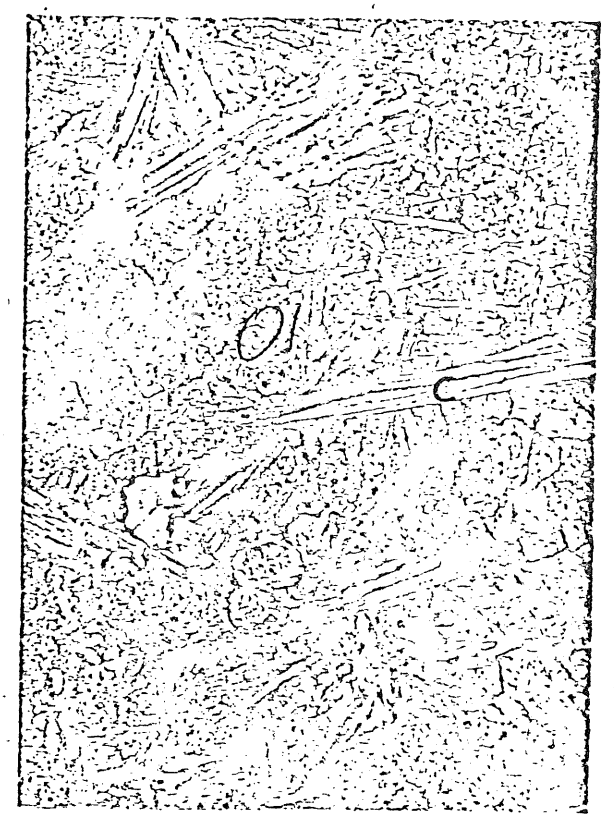

a

b